Rootletin organizes the ciliary rootlet to achieve neuron sensory function in *Drosophila*

Jieyan V. Chen,[1] Ling-Rong Kao,[1] Swadhin C. Jana,[2] Elena Sivan-Loukianova,[3] Susana Mendonça,[2] Oscar A. Cabrera,[1] Priyanka Singh,[4] Clemens Cabernard,[4] Daniel F. Eberl,[3] Monica Bettencourt-Dias,[2] and Timothy L. Megraw[1]

[1]Department of Biomedical Sciences, Florida State University, Tallahassee, FL 32306
[2]Instituto Gulbenkian de Ciência, 2780-156 Oeiras, Portugal
[3]Biology Department, University of Iowa, Iowa City, IA 52242
[4]Biozentrum, University of Basel, 4056 Basel, Switzerland

Cilia are essential for cell signaling and sensory perception. In many cell types, a cytoskeletal structure called the ciliary rootlet links the cilium to the cell body. Previous studies indicated that rootlets support the long-term stability of some cilia. Here we report that *Drosophila melanogaster* Rootletin (Root), the sole orthologue of the mammalian paralogs Rootletin and C-Nap1, assembles into rootlets of diverse lengths among sensory neuron subtypes. *Root* mutant neurons lack rootlets and have dramatically impaired sensory function, resulting in behavior defects associated with mechanosensation and chemosensation. Root is required for cohesion of basal bodies, but the cilium structure appears normal in *Root* mutant neurons. We show, however, that normal rootlet assembly requires centrioles. The N terminus of Root contains a conserved domain and is essential for Root function in vivo. Ectopically expressed Root resides at the base of mother centrioles in spermatocytes and localizes asymmetrically to mother centrosomes in neuroblasts, both requiring Bld10, a basal body protein with varied functions.

Introduction

As the major microtubule (MT)-organizing center in animal cells, the centrosome consists of a pair of MT-based centrioles that organizes a protein matrix called the pericentriolar material to regulate MT assembly. In specific cell types, the mother centriole can mature into a basal body to organize a cilium, a slender protrusion that contains an MT-based axoneme assembled from the distal tip of the basal body. Cilia generally fall into two classes: motile cilia and primary (nonmotile) cilia. Motile cilia are often present in specialized epithelia, where they beat in coordinated waves, whereas most vertebrate cells can produce a primary cilium to sense diverse extracellular signals and transduce them into important cellular responses. Disruption of cilium assembly or function causes a spectrum of diseases named ciliopathies (Goetz and Anderson, 2010; Hildebrandt et al., 2011).

In many cell types, a fibrous cytoskeletal structure called the ciliary rootlet links the base of the cilium to the cell body. Across species, the rootlet ultrastructure consists of cross-striations appearing at intervals of 50–70 nm along its length (Fawcett and Porter, 1954). The size of rootlets varies among cell types, with prominent ones, for example, in mammalian photoreceptors (Yang et al., 2002).

In mammals, Rootletin (Root, also known as ciliary rootlet coiled-coil protein) is the primary constituent of ciliary rootlets, and endogenous Root is expressed in photoreceptors and all major ciliated epithelia but absent from the spermatozoa (Yang et al., 2002, 2005). In mammalian cilia, Root resides only in the rootlet and does not extend into the basal body or cilium (Yang et al., 2002). However, the *Caenorhabditis elegans* Root orthologue, CHE-10, localizes at the proximal end of the basal body and extends into the transition zone, the most proximal region of the cilium (Mohan et al., 2013). In proliferating mammalian cells when cilia are not assembled, Root forms fibrous linkers between the centriole pairs and interacts with its paralog C-Nap1 (also known as CEP250) to promote centrosome cohesion in the cell cycle (Bahe et al., 2005; Yang et al., 2006).

The Rockefeller University Press $30.00
J. Cell Biol. Vol. 211 No. 2   435–453
www.jcb.org/cgi/doi/10.1083/jcb.201502032

JCB   435

Over decades, biologists have been intrigued by what the in vivo function of the rootlet may be. In green algae, the rootlet fibers appear to anchor the flagella and to help absorb the mechanical stress generated by flagellar beating (Hyams and Borisy, 1975; Lechtreck and Melkonian, 1991). *Root* mutant mice lack rootlets yet do not show overt defects in development, reproductive performance, or overall health, and Root is not required for normal ciliary functions during development (Yang et al., 2005). However, Root is important for the long-term stability of the cilium, particularly in specialized cells, such as photoreceptors (Yang et al., 2005). Studies in *C. elegans* showed that CHE-10 (Root orthologue) maintains cilium structure through preserving intraflagellar transport and the integrity of the transition zone and the basal body (Mohan et al., 2013). However, the role of CHE-10 may have diverged somewhat from Root in other organisms as it localizes to the basal body and transition zone of cilia and is required in neurons that lack rootlets.

Here, we identify *Drosophila melanogaster* Root as the sole orthologue of mammalian Root and C-Nap1, and show that it localizes to the ciliary rootlet in sensory neurons and, upon ectopic expression, at the proximal end of mother centrioles in spermatocytes. Root is required for neuron sensory perception, affecting various behaviors related to mechanosensation and chemosensation. Root is essential for basal body cohesion and for organizing the ciliary rootlet, and its N terminus containing the evolutionarily conserved Rootletin domain is critical for Root function and rootlet assembly in vivo.

Results

Drosophila Root is the orthologue of mammalian Rootletin and C-Nap1

Drosophila Rootletin (*Root*, *CG6129*) expresses three mRNA splice variants (Root-RE, Root-RD, and Root-RF), which differ only in their 5′UTRs and translate the same 2048–amino acid protein with a predicted molecular weight of 232.7 kD (FlyBase; St Pierre et al., 2014; Fig. 1 A). Reciprocal protein homology queries using BLAST showed Root to be the *Drosophila* orthologue of mammalian Root and C-Nap1 (Fig. 1 B). Root and C-Nap1 are paralogs in mammals, whereas *Drosophila* Root is the sole orthologue of them in *Drosophila*. These queries also revealed a "Rootletin domain" in the Root N terminus that is conserved across species (Fig. 1 B and Fig. S1 A).

To investigate the function of Root, we examined mutations associated with the *Root* locus. *Root^{MB08356}* has a *Minos* transposon insertion in the first intron of Root-RE and Root-RD but not in Root-RF (Fig. 1 A), and *Root^{MB08356}* flies did not show obvious phenotypes. To isolate new mutations in *Root*, we screened a collection of ethyl methanesulfonate–induced mutants (S. Hawley lines) using the Targeting Induced Local Lesions in Genomes (TILLING) service (Cooper et al., 2008). We isolated 17 mutant alleles: four silent mutations; 12 missense mutations, which did not show overt phenotypes (Fig. S1 B); and one nonsense mutation at amino acid 695 (K695*), which we call *Root^{66}*(Fig. 1, A and B). *Root^{66}* introduced a PspXI restriction site and resulted in a premature truncation at about one third the length of the open reading frame (Fig. 1, A and B). DNA sequencing plus genotyping by PCR-based restriction digest confirmed the nonsense mutation in *Root^{66}*(Fig. 1, C and D).

To characterize the expression pattern and subcellular localization of endogenous Root, we generated a rabbit poly-

clonal antibody against the N-terminal region of Root, which was predicted to recognize both the full-length Root and the truncated protein expressed by *Root^{66}*(Fig. 1 B). We also made a transgenic *Root* rescue construct consisting of the genomic sequence covering the entire coding region (Fig. 1 A). By tagging the construct with GFP or 6xMyc at its N terminus and fusing it to the *UAS* promoter, we generated *UAS-GFP-Root* and *UAS-Myc-Root*, whose expression could be manipulated by GAL4 "drivers" (Phelps and Brand, 1998) and monitored by the GFP signal or the Myc tag in vivo. No full-length Root protein (∼233 kD) was detected in *Root^{66}* antennae lysates, and when GFP-Root expression was driven by *elav*-GAL4, it migrated slightly slower in protein gels compared with endogenous Root (Fig. 1 E and Fig. S1 C). However, a truncated protein product predicted to be ∼77 kD from *Root^{66}* was not detected on Western blots (Fig. S1 C).

Root localizes to the ciliary rootlet in chordotonal and external sensory neurons

We examined endogenous Root expression in the peripheral nervous system (PNS) that houses type I sensory neurons, the only cell types other than sperm that have cilia (the other type, type II sensory neurons, are nonciliated and are present mainly in larvae) in *Drosophila*. Type I sensory neurons include chordotonal (Ch) and external sensory (Es) neurons. These neurons and their nearby support cells organize into the sensory organ (also called sensillum), a basic functional unit for sensing. The chordotonal organ (ChO) is an internal proprioceptor, whereas the external sensory organ (EsO) detects mechanical or chemical signals (Jarman, 2002). Depending on types, ChOs consist of a various number of scolopidia, the fundamental unit of a ChO that contains one to a few Ch neurons in addition to several accessory cells. In the Ch neuron, the cilium resides at the tip of the single prominent dendrite (Fig. 2 A).

In embryos, coimmunolabeling of Root with the PNS neuron marker 22C10/Futsch showed that Root was expressed in both Ch and Es neurons (Fig. 2, B and C). By counterstaining endogenous Root or ectopic GFP-Root with the centriole markers Pericentrin-like protein (Plp; Galletta et al., 2014), Ana1 (Blachon et al., 2009), or Centrosomin (Cnn); the transition zone marker Chibby (Cby; Enjolras et al., 2012); or the cilium markers CG11356 (Enjolras et al., 2012) and 21A6/Eys (Lee et al., 2008; Park et al., 2013), we determined that Root localized to a prominent 10- to 15-μm–long structure within the dendrite of Ch neurons, consistent with the ciliary rootlet that extends from the proximal base of the basal body, along the length of the dendrite, and terminates within the neuron cell body (Fig. 2, A and D). In addition to the rootlet, Root localized to a focus, together with Cnn and Ana1, distal to the basal body, in an unknown structure that might be the ciliary dilation (asterisks in Fig. 2 D). Thus, Root is the first known constituent of the *Drosophila* rootlet.

In *Root^{66}* embryos, Root was undetectable at the rootlet (Fig. 2 D), suggesting that the truncated protein has likely lost its function. However, in *Root^{66}*, morphologies of the neuron and the scolopale rod (which is a part of the scolopale cell that supports the neuron), as well as the localization of Cby and 21A6/Eys, appeared normal (Fig. 2 D), suggesting that the cilium structure may not be disrupted (see more details in the following paragraph). Furthermore, the truncated protein in *Root^{66}* was not detected by Western blot (Fig. S1 C), and heterozygous *Root^{66}/TM6B* did not show overt behavioral phenotypes,
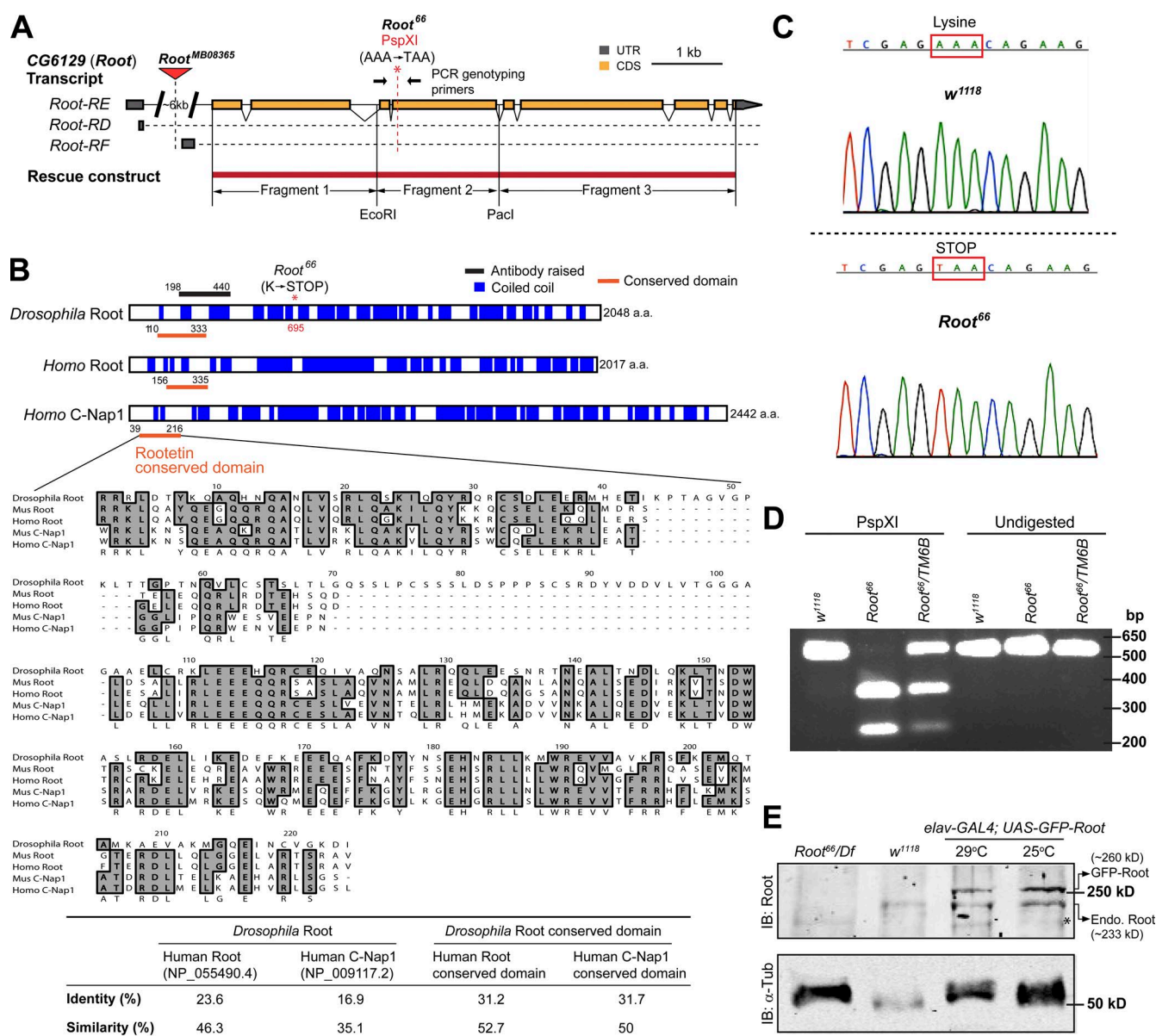
Figure 1. **Drosophila Root is the orthologue of mammalian Root and C-Nap1.** (A) Diagram showing the *Drosophila* Root transcripts RE, RD, and RF, which differ only in their 5′UTRs (only the 5′UTR is shown for RD and RF); the transposon insertion in *Root^MB08365*; the nonsense mutation in *Root^66* that also introduces a PspXI restriction site; the primers used for PCR genotyping; and the *Root* rescue construct, which was cloned by ligating three genomic fragments together. (B) *Drosophila* Root, human Root, and C-Nap1 are large proteins with extensive coiled coils, and they share a highly conserved Root domain near the N terminus. The conserved domain in mouse Root and C-Nap1 is also shown in the sequence homology. The *Root^66* mutation and the region used to raise the Root antibody are also indicated. The table shows the percentage identity and similarity between *Drosophila* Root with human Root and C-Nap1, using ClustalW alignment. (C) DNA sequencing confirms the nonsense mutation in *Root^66*. (D) PspXI restriction digest analysis of a PCR product spanning the mutation site in *Root^66*. PCR primers are as shown in A. The size of the uncut PCR products is 602 bp. DNA products amplified from wild-type *w^1118* cannot be digested by PspXI, whereas all products from the *Root^66* homozygote and about half from the *Root^66/TM6B* heterozygote are cut by PspXI into smaller fragments of expected sizes (~350 bp and 250 bp). TM6B is a balancer chromosome and is wild type for Root. (E) Western blot of isolated antenna shows that Root is absent from the *Root^66* mutant and the GFP-Root transgene expresses slightly higher levels compared with endogenous (Endo) Root. *, nonspecific bands. Lysates from 40–50 antenna pairs were loaded in each lane. *Df* is *Df(3R)Exel6197*, a deficiency line with chromosome deletion covering the entire *Root* gene. See Fig. S1 C for the whole blot. See also Fig. S1.

whereas the phenotypes of *Root^66* homozygotes were similar to *Root^66*/Df hemizygotes (see the following paragraph); therefore, *Root^66* does not appear to be dominant and may be a complete loss-of-function mutation.

We next examined Root expression in adult antennae and legs, where clustered sensory organs are found. As the auditory organ and the largest ChO in the fly, the Johnston's organ (JO) in the second antennal segment comprises arrays of more than 200 scolopidia, each containing two or three Ch neurons and a few accessory cells; the femoral chordotonal organ (fChO) in the leg consists of ~70 scolopidial units, each containing two Ch neurons (Eberl and Boekhoff-Falk, 2007; Fig. 3 A). EsOs, also known as external sensilla, typically associate with external bristles (Fig. 3 A). Immunostaining revealed that Root localized to the rootlet in Ch neurons of the JO and fChO and Es neurons of EsOs. The size of rootlets varied; Ch neurons generally had
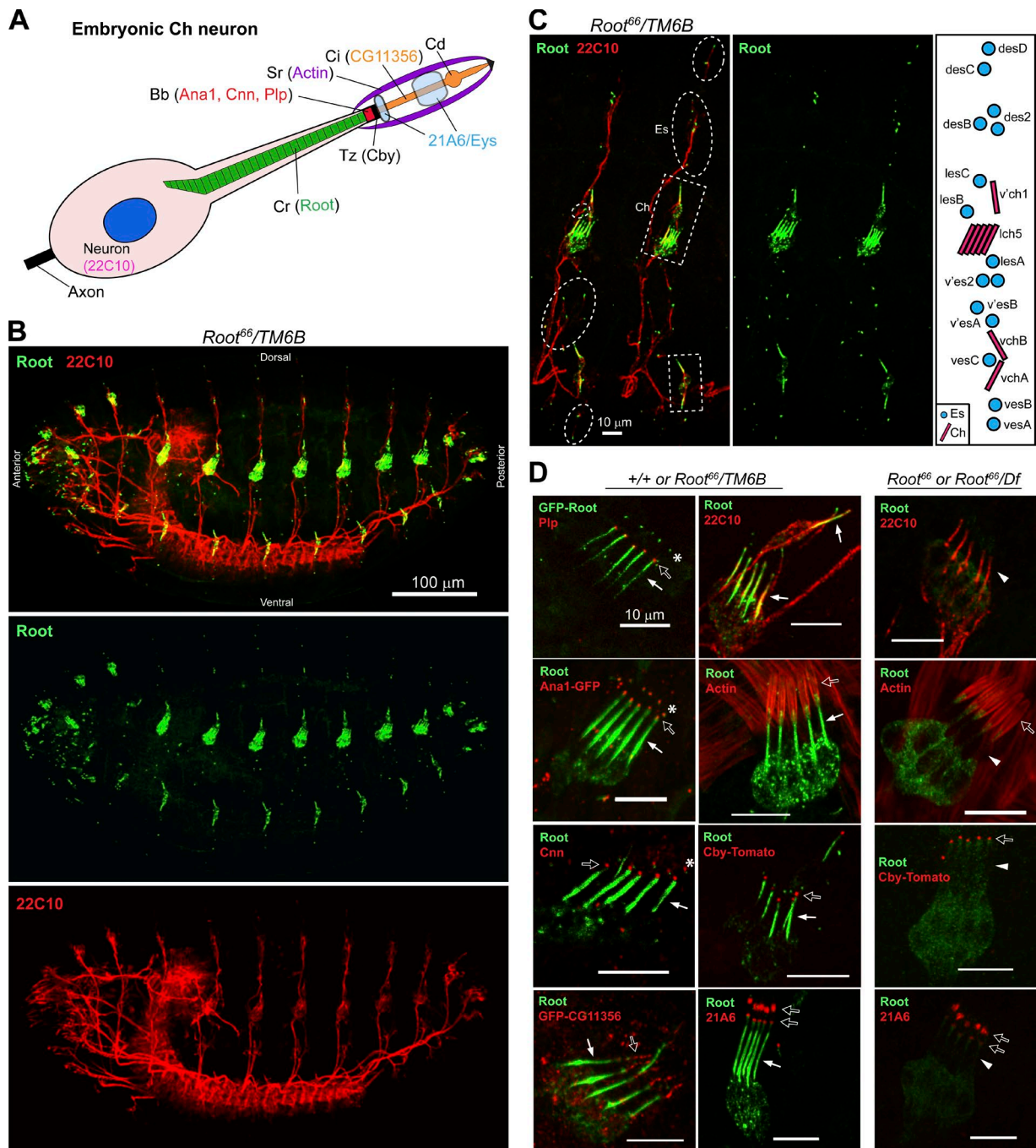
Figure 2. **Root localizes to the ciliary rootlet in embryonic Ch and Es neurons.** (A) Schematic view of the embryonic Ch neuron with structural protein markers. Bb, basal body; Cd, ciliary dilation; Ci, cilium; Cr, ciliary rootlet; Sr, scolopale rod; Tz, transition zone. (B) Endogenous Root is expressed in the embryonic PNS. Antibody 22C10 recognizes Futsch, a PNS neuron marker. (C) Root is expressed in both Ch and Es neurons. Boxed and circled areas indicate Ch neurons and Es neurons, respectively, which are illustrated as pink bars and blue circles in the cartoon on the right. The schematic is adapted from Orgogozo and Grueber (2005) and the names of type I sensory neurons are indicated. (D) Root localizes to the rootlet in Ch neurons. Endogenous Root or GFP tagged Root is counterstained with the PNS marker 22C10 or the following ciliary markers (open arrows): Plp, Ana1, and Cnn mark the Bb; Cby marks the Tz; CG11356 marks the axoneme; and 21A6/Eys marks the cilium proximal end and the extracellular region right below the ciliary dilation. Root also localized to a focus, together with Cnn and Ana1, distal to the basal body, in an unknown structure that might be the ciliary dilation (asterisks). In control +/+ or Root[66]/TM6B, Root resides at a structure consistent with the ciliary rootlet (solid arrows) that extends from the base of the basal body, passes through the dendrite, and reaches the cell body. In homozygous Root[66] or hemizygous Root[66]/Df, Root is absent from the rootlet (solid arrowheads). However, the morphologies of mutant neurons and scolopale rods appear normal, as marked by 22C10 and actin, respectively; the localizations of Cby and 21A6 are also unaffected (open arrows). Mutant embryos are from Root heterozygous parents and distinguished by Root antibody staining. Bars: (B) 100 µm; (C and D) 10 µm.
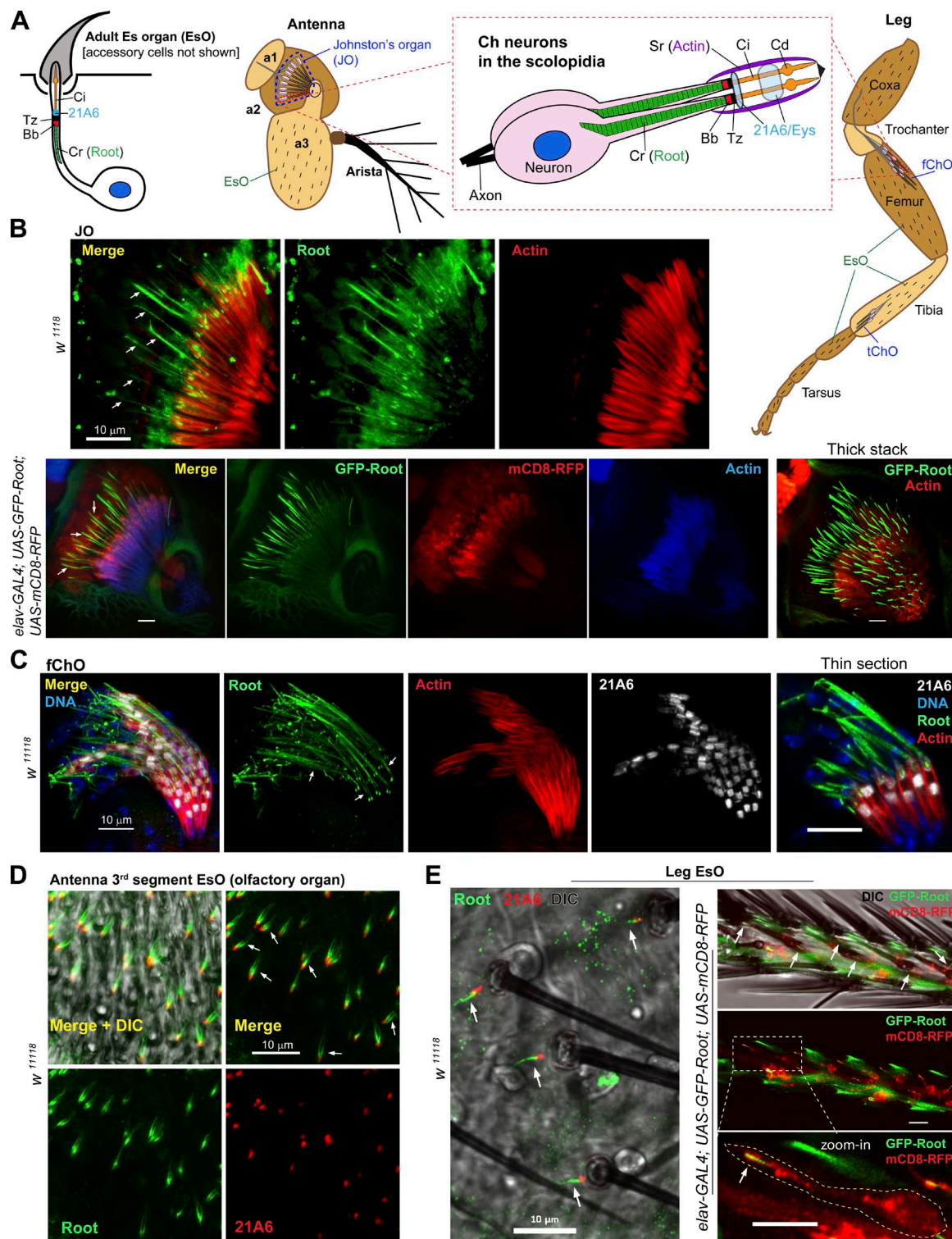
Figure 3. **Root localizes to the ciliary rootlet in adult Ch and Es neurons.** (A) Illustration of ChOs and EsOs in the antenna and leg. The JO in the antennal a2 segment is a specialized ChO composed of arrays of scolopidia, each containing two or three neurons. In the leg, scolopidia, each containing two neurons, are present in bundles in the fChO and tChO. EsOs, consisting of Es neurons and supporting cells, usually associate with external bristles. Bb, basal body; Cd, ciliary dilation; Ci, cilium; Cr, ciliary rootlet; Sr, scolopale rod; Tz, transition zone. (B) In Ch neurons of the JO, endogenous Root (upper panel) or GFP-Root (bottom panel) localizes to the ciliary rootlet, typically 15–25 µm long. The rootlet stretches from the base of the cilium to the neuron cell body (arrows). Upper panel shows immunostaining of antenna cryosections. Actin marks scolopale rods; mCD8-RFP localizes to plasma membranes and outlines the neurons. (C) Endogenous Root localizes to the approximately 20-µm rootlet in Ch neurons of the fChO. Each scolopidium has two Ch neurons and hence two rootlets (arrows). Actin marks scolopale rods, 21A6 marks the cilium base and the region right below the ciliary dilation. (D) Endogenous Root resides at the ~2- to 10-µm rootlet in Es neurons (olfactory neurons) in the antennal a3 segment. Each set of olfactory organs has one to four neurons, as indicated by different numbers of rootlets. 21A6 marks the cilium base. (E) In leg Es neurons, endogenous Root (left) or GFP-Root driven by *elav*-GAL4 (right) localizes at the ~2- to 8-µm rootlet. 21A6 marks the cilium base, mCD8-RFP outlines the neurons. Bars, 10 µm.

longer rootlets at 15–25 µm in length, whereas Es neurons had ones that were 2–10 µm long (Fig. 3, B–E).

Root is essential for neuronal sensory responses

Although viable, *Root[66]* mutant flies were moderately uncoordinated, a phenotype commonly associated with defects in neuron mechanosensation (Kernan et al., 1994). *Root[66]* flies also showed little, if any, startle response (Video 1); they would frequently fall over onto their side or back while traversing the surface of an agar plate and would occasionally experience what appear to be seizures. These observations, together with the localization of Root to rootlets and the indication from previous studies that rootlets are linked to cilium function, led us to test the environmental sensing capabilities of *Root[66]* flies with a series of behavioral assays.

Flies exhibit negative geotaxis behavior, the innate ability to climb against gravity, which is governed by two aspects: gravity perception and the locomotor coordination (Gargano et al., 2005; Rhodenizer et al., 2008; Enjolras et al., 2012). Gravity is mainly perceived by the JO, analogous to the role of the inner ear for balance in humans (Kamikouchi et al., 2009; Sun et al., 2009), whereas locomotor coordination is primarily achieved by EsOs, with some contribution from ChOs (other than the JO) required for proprioception (Kernan et al., 1994; Enjolras et al., 2012). The negative geotaxis assay showed that *Root[66]* flies, as well as flies with Root knockdown by RNAi in the nervous system, had severe defects in climbing (Fig. 4, A and B; and Fig. S2 A), indicating disruption of neuronal functions in the JO and/or EsOs. This climbing defect is likely due to a lack of motor coordination caused by Root-deficient neurons. Rescue of *Root[66]* by expressing GFP-Root in different parts of the nervous system with specific GAL4 drivers (Fig. 4 A) established that both JO and EsO functions in *Root[66]* mutant were impaired. GFP-Root expression in both the JO and EsOs driven by *elav*- or *Insc*-GAL4 restored the performance to a level similar to that in controls, whereas expression restricted to mainly ChOs (including the JO) by *tilB*-GAL4 + *nan*-GAL4 or to the JO by *JO15-2*-GAL4 rescued the phenotype partially but significantly (Fig. 4 B). Meanwhile, the central nervous system (CNS) does not require Root for negative geotaxis behavior because GFP-Root driven by *wor*-GAL4 failed to rescue the *Root[66]* phenotype (Fig. 4 B). Collectively, Root expression in ChOs and EsOs is essential for locomotor coordination and hence negative geotaxis behavior.

In larvae, ChO sensilla are the major sensory components for touch sensitivity, whereas EsOs also contribute to sensing touch (Caldwell et al., 2003). Root localized to rootlets in ChOs and EsOs of the developing embryos (Fig. 2, B–D). We used a touch sensitivity assay, which showed that physical object sensing in larvae requires Root, and *Root[66]* was most effectively rescued by GFP-Root expression in both ChOs and EsOs (Fig. 4 C). The rescue experiment also revealed the major role of Root in ChOs for touch responsiveness, as shown by the significant although not complete rescue by GFP-Root expression from the *tilB*-GAL4 + *nan*-GAL4 driver (Fig. 4 C).

To measure the chemosensory capabilities of *Root[66]* flies, we performed the proboscis extension reflex assay to assess their gustatory response. Root is required for normal chemosensation because *Root[66]* flies showed reduced taste perception of sucrose and the phenotype was rescued by expressing GFP-Root in the PNS (Fig. 4 D). Interestingly, females and males showed different gustatory behavioral responses to sucrose, and the rescue was more thorough in females than in males (Fig. 4 D).
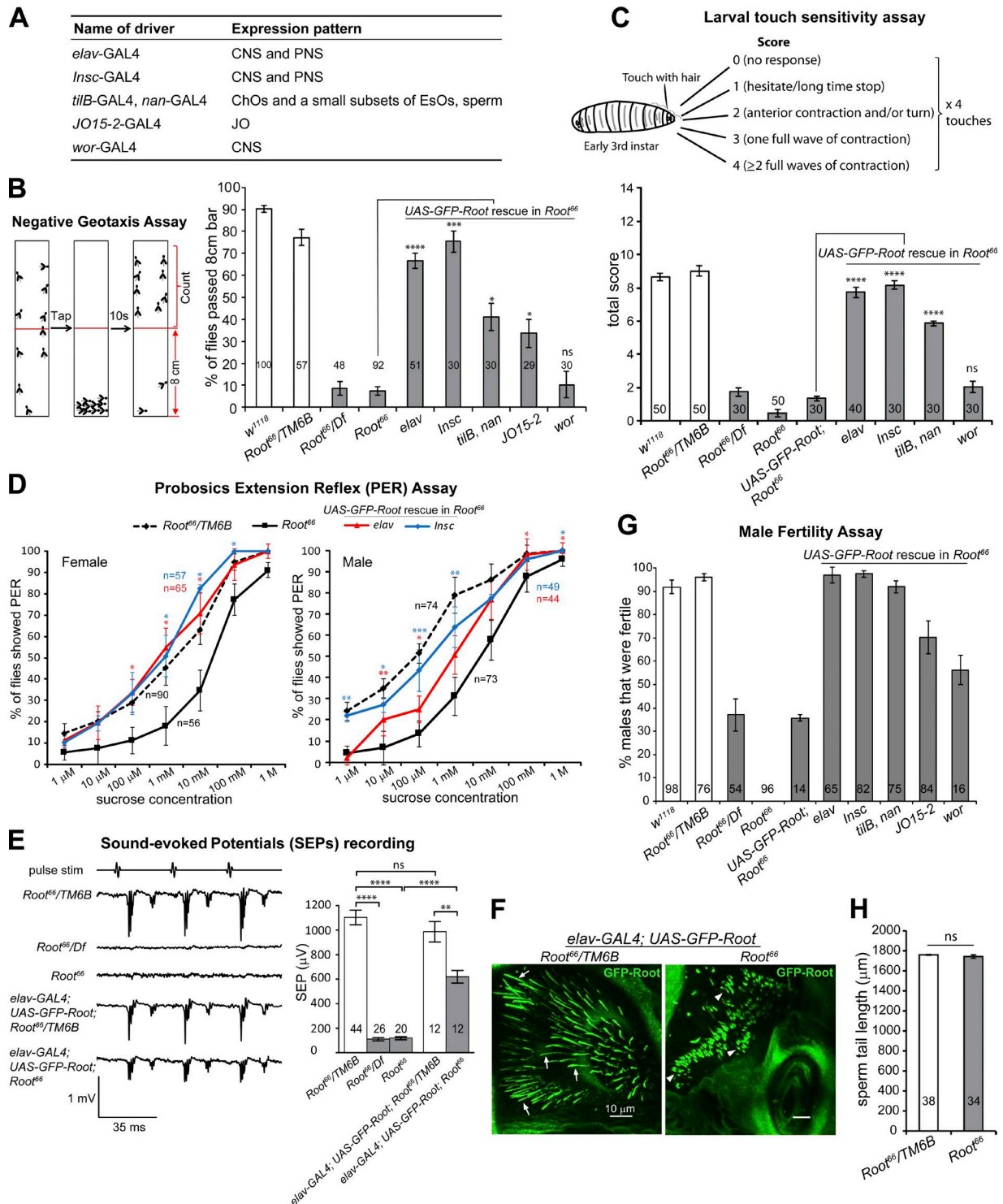
Hearing in flies is achieved by the JO, the insect auditory organ. Because Root localizes to long rootlets in JO neurons (Fig. 3 B), and our behavior tests showed the importance of Root in neuron functions (Fig. 4, B–D), we measured the hearing capability of *Root[66]* flies. Indeed, *Root[66]* flies were deaf, as shown by electrophysiologic recordings of sound-evoked potentials (SEPs) in the JO. Hearing impairment was rescued by pan-neuronal expression of GFP-Root; however, the SEP amplitude in *Root[66]*-rescued JOs was not fully restored to that of the control (Fig. 4 E). Consistent with the partial restoration of hearing, we found that in the *Root[66]* mutant background GFP-Root supported the assembly of much shorter rootlets in ChOs (both JO and fChO) relative to controls (Fig. 4 F and Fig. S2 B). In contrast, the rootlets in *Root[66]*-rescued EsOs appeared normal (Fig. S2 B). The shorter rootlets are not due to insufficient expression of GFP-Root because Western blot showed that the level of GFP-Root was slightly higher than that of endogenous Root (Fig. 1 E). Insufficient rescue is not likely because of interference from the truncated protein encoded by *Root[66]*, as GFP-Root in the *Root[66]/TM6B* heterozygous background revealed normal-sized rootlets in ChOs (Fig. 4 F and Fig. S2 B). Moreover, expression of Root with a different N-terminal tag (UAS-Myc-Root) also rescued *Root[66]* and also formed shorter-than-normal rootlets in ChOs (not depicted). Tagging the N terminus of Root might partially interfere with its assembly into long rootlets. Importantly, however, this phenomenon suggests that forming a rootlet, even a short one, restores Ch neuron functions significantly, indicating that the essential role of Root is associated with rootlet assembly.

We also found that *Root[66]* males had impaired fertility (Fig. 4 G). Inspection of *Root[66]* testes revealed that the seminal vesicles were of normal size and contained motile sperm with normal tail length (Fig. 4 H), indicating that the sperm are likely capable of fertilizing eggs. This led us to suspect that *Root[66]* males might have defects in the nervous system that impaired mating-related behaviors, which was substantiated by the rescue of male fertility through GFP-Root expression in the PNS (Fig. 4 G).

Altogether, these behavioral experiments demonstrate that Root is essential for peripheral neurons to exert mechanosensation (negative geotaxis, touch sensitivity, and hearing) and chemosensation (gustatory perception), likely by affecting cilium function in sensory neurons by regulating rootlet assembly (see the following paragraph).

The Rootletin conserved domain is essential for Root protein function in vivo

It has been proposed that the N terminus of mammalian Root is a globular domain, whereas the remainder of the protein assembles into a coiled-coil filament (Yang et al., 2002). The N-terminal 533 amino acids were shown to bind to several kinesin light chains, suggesting that kinesin 1 might link MTs to the rootlet via the conserved globular domain (Yang and Li, 2005). To determine the in vivo function of Root N terminus, we deleted the N-terminal 333 amino acids covering the Rootletin conserved domain to generate the mutant RootDEL, which was then tagged with RFP and expressed in flies (Fig. 5 A and Fig. S2 C). RFP-RootDEL failed to rescue the locomotor (negative geotaxis) and touch sensitivity defects in *Root[66]* flies or larvae (Fig. 5, B and C). RFP-RootDEL localized to rootlets in control

A

Name of driver	Expression pattern
elav-GAL4	CNS and PNS
Insc-GAL4	CNS and PNS
tilB-GAL4, *nan*-GAL4	ChOs and a small subsets of EsOs, sperm
JO15-2-GAL4	JO
wor-GAL4	CNS

B

Negative Geotaxis Assay

Tap → 10s → Count / 8 cm

% of flies passed 8cm bar

UAS-GFP-Root rescue in *Root^66^*

100 — w^{1118}
57 — *Root^66^/TM6B*
48 — *Root^66^/Df*
92 — *Root^66^*
51 — *elav* ****
30 — *Insc* ***
30 — *tilB, nan* *
29 — *JO15-2* *
30 — *wor* ns

C

Larval touch sensitivity assay

Touch with hair
Early 3rd instar

Score:
- 0 (no response)
- 1 (hesitate/long time stop)
- 2 (anterior contraction and/or turn)
- 3 (one full wave of contraction)
- 4 (≥2 full waves of contraction)
x 4 touches

total score

UAS-GFP-Root rescue in *Root^66^*

50 — w^{1118}
50 — *Root^66^/TM6B*
30 — *Root^66^/Df*
50 — *Root^66^*
30 — *UAS-GFP-Root; Root^66^*
40 — *elav* ****
30 — *Insc* ****
30 — *tilB, nan* ****
30 — *wor* ns

D

Probosics Extension Reflex (PER) Assay

- - ◆ - - *Root^66^/TM6B*   —■— *Root^66^*
UAS-GFP-Root rescue in *Root^66^*: —●— *elav* (red)   —◆— *Insc* (blue)

Female: % of flies showed PER vs sucrose concentration (1 μM, 10 μM, 100 μM, 1 mM, 10 mM, 100 mM, 1 M)
n=57, n=65, n=90, n=56

Male: % of flies showed PER vs sucrose concentration
n=74, n=73, n=49, n=44

E

Sound-evoked Potentials (SEPs) recording

pulse stim
Root^66^/TM6B
Root^66^/Df
*Root^66^*
elav-GAL4; UAS-GFP-Root; Root^66^/TM6B
*elav-GAL4; UAS-GFP-Root; Root^66^*

1 mV / 35 ms

SEP (μV)

ns / **** / **** / **** / **

44 — *Root^66^/TM6B*
26 — *Root^66^/Df*
20 — *Root^66^*
12 — *elav-GAL4; UAS-GFP-Root; Root^66^/TM6B*
12 — *elav-GAL4, UAS-GFP-Root; Root^66^*

F

elav-GAL4; UAS-GFP-Root
Root^66^/TM6B — GFP-Root
*Root^66^* — GFP-Root
Scale bars 10 μm

G

Male Fertility Assay

UAS-GFP-Root rescue in *Root^66^*

% males that were fertile

98 — w^{1118}
76 — *Root^66^/TM6B*
54 — *Root^66^/Df*
96 — *Root^66^*
14 — *UAS-GFP-Root; Root^66^*
65 — *elav*
82 — *Insc*
75 — *tilB, nan*
84 — *JO15-2*
16 — *wor*

H

sperm tail length (μm)
ns

38 — *Root^66^/TM6B*
34 — *Root^66^*

Figure 4. **Root is essential for neuron-specific behaviors.** (A) GAL4 drivers used for *Root* rescue and their expression patterns. (B) Root is essential for negative geotaxis. The percentages of *Root^66^* mutant flies that passed the negative geotaxis assay are significantly lower compared with controls (white bars). The mutants are rescued, to different degrees, by expressing GFP-Root with different GAL4 drivers. Expression in the entire nervous system (*elav*, *insc*) or mainly in the ChOs (*tilB+nan*, *JO15-2*) conferred complete or significant rescue, whereas expression limited to the central nervous system (CNS; *wor*) did not. (C) *Root^66^* larvae lack sensitivity to touch, compared with the controls (white bars). Touch sensitivity is best restored by expressing GFP-Root in both ChOs and EsOs (*elav*, *insc*), expression limited to mainly ChOs (*tilB+nan*) also rescues the defect significantly, but expression of GFP-Root in CNS (*wor*) did not rescue the phenotype. (D) *Root^66^* flies show reduced taste responses to sucrose compared with *Root^66^/TM6B*. The proboscis extension reflex (PER) taste response is significantly restored by driving GFP-Root expression in the entire PNS (*elav*, *Insc*), although the rescue was more thorough in females than in males. Significance was measured between *Root^66^* and rescue groups at each sucrose concentration. (E) *Root^66^* flies show significantly reduced hearing response indicated by SEPs, compared with *Root^66^/TM6B* (white bars). GFP-Root expression driven by *elav*-GAL4 rescues the hearing impairment of *Root^66^* significantly but not completely. (F) In the JO, ectopically expressed GFP-Root localizes to the normal-sized, ~15- to 25-μm rootlets in *Root^66^/TM6B* (arrows); however, the GFP-Root rescue in the *Root^66^* mutant organizes much shorter rootlets at ~2–8 μm (arrowheads). Bars, 10 μm. (G) *Root^66^* males have impaired fertility. More than 90% of the control males are fertile (white bars); in contrast, none of *Root^66^* and less than 40% of *Root^66^/Df* males produce

neurons; however, in *Root[66]* neurons, it localized to basal bodies as foci but failed to assemble into rootlets in both Ch and Es neurons (Fig. 5, D and E). These results show that the conserved Root domain is required for normal rootlet assembly and Root function but is separable from its localization to basal bodies, suggesting that localization to the basal body is not sufficient for Root activity but rather the assembly of a rootlet is critical for ciliary function.

Root is essential for rootlet formation and cohesion of basal bodies

Ultrastructural studies of JO neurons by electron microscopy revealed that *Root[66]* mutants lacked the striated rootlets that normally extend from the basal body (Fig. 6, A–C), confirming the essential role of Root in striated rootlet assembly in vivo. Furthermore, the connecting fibers between the proximal basal body (pBB) and the distal basal body (dBB) were also lost in the mutant (Fig. 6, A and D). In *Root[66]* Ch neurons, we observed electron-dense masses that appeared to accumulate at the base of the cilium (Fig. 6 B), perhaps an aberrant rootlet or the result of abnormal accumulation of biomolecules that normally traffic between the dendrite and the cilium. Alternatively, because the head domain at the N terminus of Root was proposed to form the electron-dense striations in the rootlet polymer by EM (Yang et al., 2002), perhaps the truncated protein expressed from *Root[66]* is aggregating into an aberrant striation structure. However, our antibody, which is predicted to recognize this domain, did not detect the truncated protein by Western blot (Fig. S1 C) or by immunostaining the puncta that might be expected on the basis of the EM images.

Because Root and C-Nap1 are known to regulate centrosome cohesion in mammalian cells (Bahe et al., 2005; Yang et al., 2006), we measured the distance between the pBB and dBB in *Root[66]* Ch neurons from transmission EM images. Basal bodies in wild-type JO neurons had an average separation of 300.5 nm, with small variance (± 69.4 nm; Fig. 6 E). In *Root[66]*, although the mean distance between basal bodies was not significantly different from wild type, it is significantly more variable: 381.3 ± 236 nm (Fig. 6 E). In addition, 60% of *Root[66]* JO neurons apparently lost the pBB as examined by EM serial sections (Fig. 6 D). Immunostaining of Root in olfactory neurons (Es neurons) of the antennal third segment showed that the localization of Root also extended into the space between the pBB and dBB, which we assume to be the connecting fibers (Fig. 6 F). Consistent with the EM data, confocal imaging of Ana1, which localizes to both basal bodies, showed that the pBB was significantly separated from the dBB in *Root[66]* olfactory neurons, as we observed significantly higher frequency of isolated "free" centrioles in the mutant (Fig. 6, G and H).

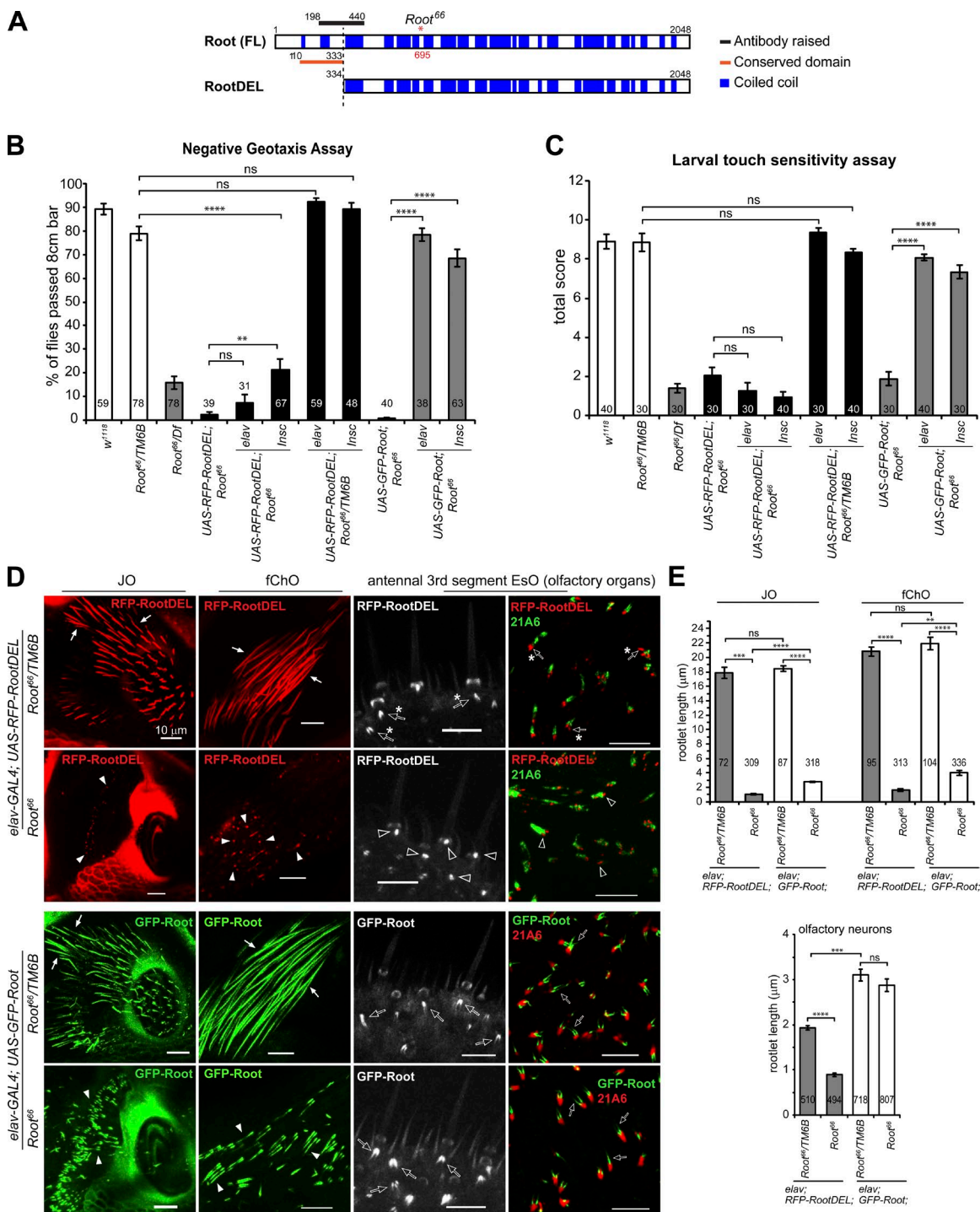## The cilium structure appears normal in the *Root[66]* mutant

As stated above, in the *Root[66]* embryonic PNS, there were neither overt morphological defects in the Ch neuron or the scolopale rod nor localization defects of the transition zone protein Cby or the ciliary p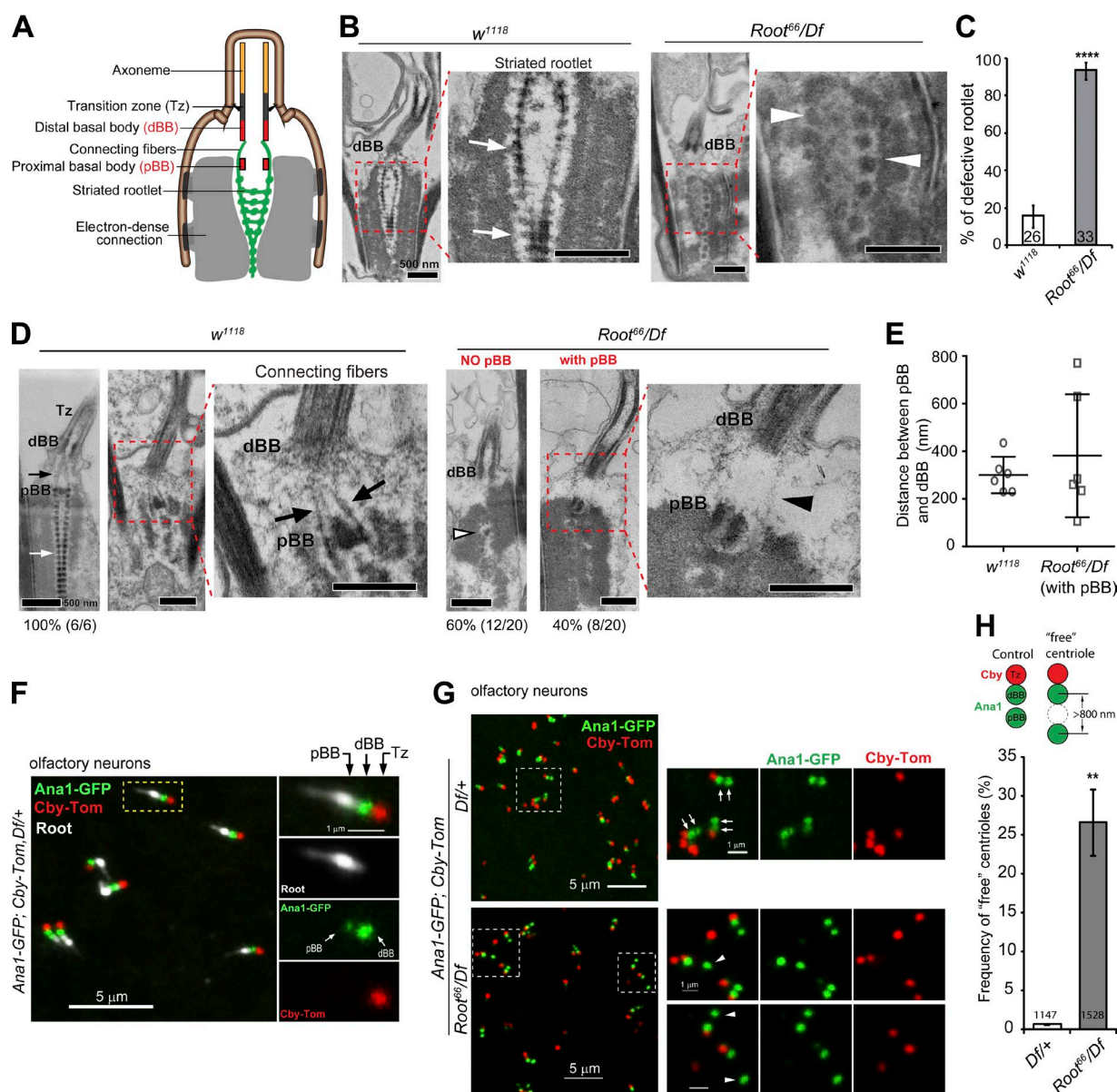rotein 21A6/Eys (Fig. 2 D). We further investigated cilium morphology in adults by expressing mCD8-GFP to outline the neuron cell membranes, including the ciliary membranes. We found that the morphology of JO and fChO cilia appeared normal in *Root[66]* (Fig. 7 A). We also examined the olfactory neurons in the antenna, as well as the "isolated" Es neurons in the arista (three "cold cell neurons" and three "hot cell neurons," which act as thermoreceptors; Foelix et al., 1989; Gallio et al., 2011; Ni et al., 2013) and found that the cilium morphology in these neurons from *Root[66]* mutant were similar to the control (Fig. 7 A). Because cilia appeared to degenerate in *C. elegans Che-10* (*Root* orthologue) and mouse *Root* mutants with age (Yang et al., 2005; Mohan et al., 2013), we compared the cilia in young flies with those aged 20 and 40 d and found no obvious changes in cilium integrity (Fig. 7 A). Additionally, the transition zone maker Cby and cilium marker 21A6/Eys appeared normal with aging (Fig. 7, B and C; and Fig. S3, A and B). Moreover, the cilium axoneme ultrastructure in mutant JO neurons also appeared intact by EM imaging (Fig. 7 D). Thus, it is likely that the behavioral phenotypes associated with *Root* loss of function are due not to a gross disruption of cilium structure but rather a disruption of cilium function or the transmission of sensory signaling between the cilium and the neuron. Therefore, cilia in the *Root[66]* mutant appear morphologically normal and do not degenerate as they age, and we conclude that cilium assembly and maintenance do not require functional Root or an intact rootlet in *Drosophila*.

The centriole, but not the cilium, is required for normal ciliary rootlet assembly

We next sought to determine whether rootlet assembly requires the centriole (basal body), with which the rootlet has an intimate association in all species examined, or requires other basal body components. We found that in *Sas-4* mutant, in which most cells lack centrioles (Basto et al., 2006), rootlet assembly in Es neurons was abolished because little or no Root was detected at rootlet regions (Fig. 7 E). Similarly, rootlets were absent in most *Sas-4* Ch neurons in the JO, although we detected a few rootlet-like structures (Fig. S3 C). Mutations in other centriole biogenesis proteins, Sas-6 and Asterless (Asl; Rodrigues-Martins et al., 2007; Varmark et al., 2007), also showed a loss of rootlet formation in olfactory neurons (Fig. S3 D). However, mutant disruption of Cnn, Spd-2, Plp, or Bld10/CEP135, which are not required for centriole biogenesis but in some cases affect locomotor function (Plp and Spd-2; Martinez-Campos et al., 2004; Dix and Raff, 2007; Giansanti et al., 2008; Mottier-Pavie and Megraw, 2009; Carvalho-Santos et al., 2012), did not overtly impair rootlet formation (Fig. S3 D). Interestingly, in *Plp* mutant neurons that lack cilia (Martinez-Campos et al., 2004) and the basal bodies are displaced from the dendrite tip (Galletta et al., 2014), rootlets seemed to assemble efficiently on the detached basal bodies, as most of them were not associated with the cilium base (or the dendrite tip in this case) marked with 21A6/Eys (Fig. 7 F). This shows that rootlets can assemble at basal bodies even when cilia are absent. Together, these findings indicate that Root directs rootlet assembly in a centriole-dependent but cilium-independent fashion.

---

progeny. *UAS-GFP-Root; Root[66]* showed some fertility, probably because of leaky expression of the transgene. The fertility of *Root[66]* males is fully rescued by expressing GFP-Root in the nervous system with *elav-*, *Insc-*, or *tilB+nan-*GAL4. (H) *Root[66]* males produce mature sperm with normal tail length. For all charts, numbers of flies/larvae/sperm assayed are indicated in/near the bars, and error bars represent SEM. ns, P > 0.05; *, $P \leq 0.05$; **, $P \leq 0.01$; ***, $P \leq 0.001$; ****, $P \leq 0.0001$. See also Video 1 and Fig. S2.

Figure 5. **The Rootletin conserved domain is essential for Root function and rootlet assembly, but not for localization to basal bodies.** (A) Schematic view showing RootDEL, which has a deletion of the N-terminal 333 amino acids, including the entire conserved Root domain. (B) *elav*-GAL4 driving RFP-RootDEL expression does not rescue *Root⁶⁶* locomotor defects. Flies with RFP-RootDEL expression driven by *Insc*-GAL4 performed better than the *Root⁶⁶*, but the level of rescue is low compared with that of GFP-Root (full length). RootDEL does not introduce dominant effects, as flies with RFP-RootDEL expression in the *Root⁶⁶/TM6B* background do not show locomotor defects. (C) RFP-RootDEL expression driven by *Insc-* or elav-GAL4 failed to rescue the larval touch insensitivity phenotype in *Root⁶⁶*. RFP-RootDEL expression in *Root⁶⁶/TM6B* background does not cause defects, indicating no dominant effects are associated with RootDEL. (D) RFP-RootDEL localizes to basal bodies but does not assemble normal rootlets. GFP-Root is included as a positive control. When expressed in control *Root⁶⁶/TM6B* Ch neurons, RFP-RootDEL localizes to rootlets and does not affect their assembly (solid arrows in top panels), similar to GFP-Root (solid arrows in lower panels). For unknown reason, in *Root⁶⁶/TM6B* Es neurons, RootDEL localizes to rootlets shorter than those labeled by GFP-Root (open arrows with asterisks), see also E. While GFP-Root supports assembly of short rootlets in *Root⁶⁶* Ch neurons (solid arrowheads) and normal ones in Es neurons (open arrows), RFP-RootDEL localizes to basal bodies but does not form proper rootlets in both Ch and Es neurons (solid and empty arrowheads). Note that the signal of RFP-RootDEL may not be a proper rootlet but rather a focus of RFP-RootDEL accumulated at the basal body. The black and white panels are live images of the signal for GFP-Root or RFP-RootDEL taken through the pupal cuticle. Bars, 10 µm. (E) Quantification of rootlet lengths in control and *Root⁶⁶* neurons expressing GFP-Root or RFP-RootDEL. Rootlets are measured from at least four antennae for each genotype. Rightmost panels in D show images of the antenna squash. For all graphs, numbers of males/larvae/rootlets assayed are indicated in/near the bars, and error bars represent SEM. ns, P > 0.05; **, P ≤ 0.01; ***, P ≤ 0.001; ****, P ≤ 0.0001. See also Fig. S2.

Figure 6. **Root is essential for rootlet formation and basal body cohesion.** (A) Schematic view of the rootlet and its connection to the basal bodies in the JO. (B) $Root^{66}$ JO neurons lack striated rootlets. Representative transmission EM longitudinal section images show that in control w^{1118}, the rootlet is organized as a characteristic striated fiber (arrows), but in $Root^{66}/Df$, this organization is lost; instead, some disconnected electron-dense clumps are observed at the rootlet region (arrowheads). (C) Quantification of defective rootlets in $Root^{66}$ JO. Rootlet structures were observed in longitudinal and cross-sections. Numbers of rootlets analyzed are indicated; ****, P $\leq$ 0.0001. (D) The connecting fibers are normally found between the pBB and the dBB as thread-like electron-dense structures in the control (black arrows); they are lost in $Root^{66}$ (black arrowhead). The striated rootlet is present in wild type (white arrow) but disrupted in the mutant (white arrowhead). Examined by serial sections, 60% of mutant JO neurons appear to lack a pBB. (E) Quantification of the edge-to-edge distance between the dBB and pBB in JO Ch neurons. Single data points, mean, and standard deviation are indicated. There is no significant difference between mean values of w^{1118} and $Root^{66}$, using Mann-Whitney test. But F-distribution analysis indicated that distances in $Root^{66}$ are significantly more variable than in w^{1118}. (F) Immunostaining of olfactory neurons for basal bodies (Ana1-GFP), the transition zone (Cby-Tomato), and Root. Root localizes into the space between dBB and pBB. (G) In the control olfactory neurons (upper panels), basal bodies (Ana1-GFP) are in tandem pairs (arrows) with Cby located near one of them. In $Root^{66}$ (lower panels), one of the basal bodies is frequently more distant, or "free" (arrowheads). (H) Quantification of loss of basal body cohesion in $Root^{66}$. A basal body (centriole), marked with Ana1-GFP, is scored as "free" if it is not directly associated with the Tz (Cby-Tomato) and located more than 800 nm (center-to-center distance, which is about twice the diameter of an Ana1-GFP dot) from the nearest dBB that is associated with Cby. The frequency of "free centrioles" is defined by the ratio of the number of "free" Ana1 dots to the number of Cby dots. Numbers near/in the bars indicate numbers of Cby dots assayed from at least four antennae for each genotype. **, P $\leq$ 0.01. F and G show images of the antenna squash. Bars: (B and D) 500 nm; (F and G) 5 µm; (F and G, zoom) 1 µm.

Ectopic Root localizes to mother centrioles in testes and distributes asymmetrically to neuroblast centrosomes

In the Kc167 cell line which is derived from the *Drosophila* late embryo (Cherbas et al., 1988), ectopic expression of Root in-

duced assembly of rootlet-like fibers that were associated with the centrioles but not with MTs (Fig. 8 A), suggesting that Root has the potential to organize rootlets even in nonciliated cells.

Drosophila Root, as the orthologue of mammalian Root and C-Nap1, behaves like both proteins, depending on the cell
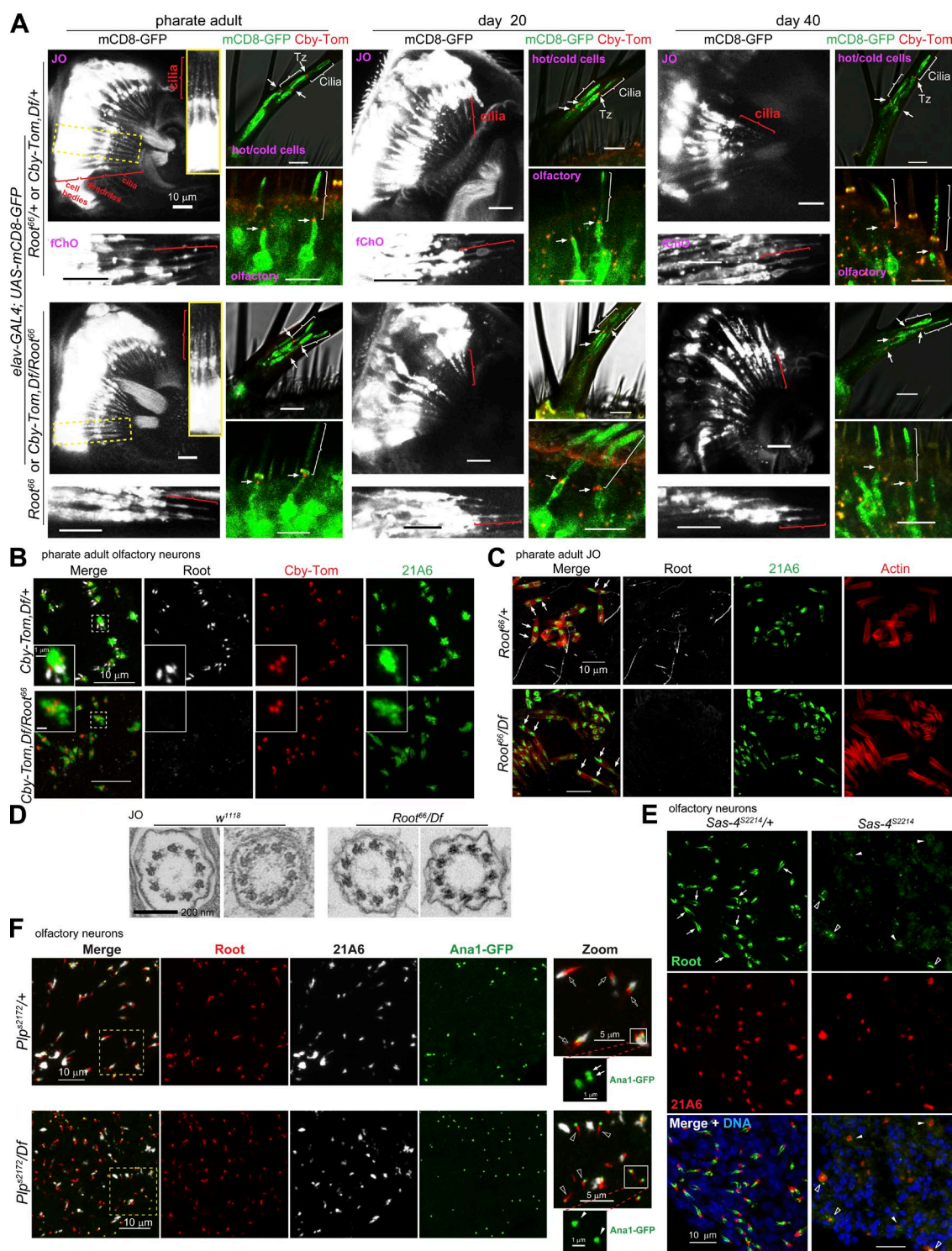
Figure 7. **Cilium structure is normal and maintained with age in *Root* mutant neurons, and centrioles but not cilia are required for rootlet assembly.** (A) Various ciliated neurons at indicated age expressing mCD8-GFP to label ciliary membranes and Cby-Tomato to mark the transition zone (Tz). Brackets indicate the cilia, and arrows the Tz. Cilium morphology appears normal in *Root*[66] through aging. hot/cold cells: temperature-sensing neurons in the arista, olfactory: olfactory neurons in the antennal third segment. For the hot/cold neuron images, transmitted light images are overlaid to show the morphology of the arista. (B) Olfactory neurons stained for 21A6 to label the cilium base and Cby-Tom to label the Tz. Cby and 21A6 localizations appear normal in *Root*[66]. (C) Ch neurons in the JO stained for actin to label the scolopale rods and 21A6 to label cilia. 21A6 localizes both to the cilium base and a distal region in the cilium (arrows), and this localization appears normal in *Root*[66]. (D) Cross-section of JO cilia by transmission electron microscopy shows that *Root*[66] axoneme ultrastructure appears normal. (E) *Sas-4* mutant lacking centrioles fails to organize rootlets in olfactory neurons. Compared with the control, where rootlets project from cilium base marked by 21A6 (arrows), rootlet structures are absent in most *Sas-4* olfactory neurons (solid arrowheads), although sometimes abnormal tiny fibers are associated with 21A6 (open arrowheads). Endogenous Root is stained in green. (F) In control olfactory neurons, all rootlets are associated with the cilium base marker 21A6 (empty arrows), and the basal bodies (dBB and pBB) marked by Ana1-GFP are in tandem (solid arrows). In *Plp* mutant that lacks cilia and has the basal bodies displaced from the dendrite tip, most of the rootlets (empty arrowheads) are associated with a single basal body (solid arrowheads), which is not attached with 21A6. B, C, E, and F show images of the antenna squash. Bars: (A–C and E) 10 µm; (B, inset) 1 µm; (D) 200 nm; (F, main) 10 µm; (F, zoom) 5 µm; (F, zoom inset) 1 µm. See also Fig. S3.
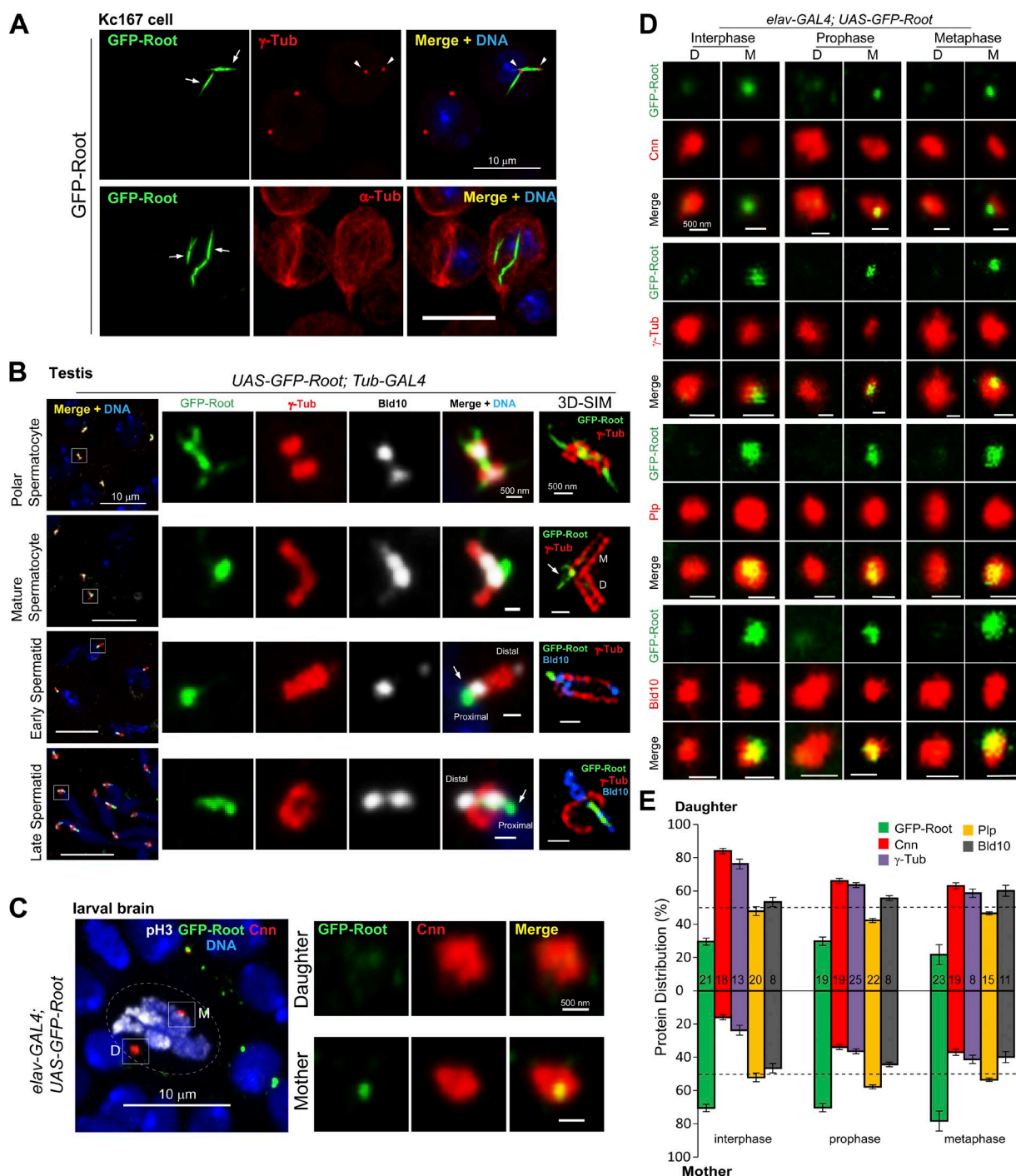
Figure 8. Ectopic Root localizes to mother centrioles in testes and distributes asymmetrically to NB centrosomes. (A) Ectopic expression of Root in Kc167 cells forms rootlet-like fibers (arrows) that associate with the centrioles marked by γ-Tub (arrowheads) but not the MTs marked by α-Tub. (B) During spermatogenesis, GFP-Root associates with centrioles and has localization patterns that vary with cell type. In polar spermatocytes, GFP-Root forms fibrous structures both inside and between the centriole pairs. In mature spermatocytes, which have long, engaged centriole pairs, GFP-Root localizes at the base of the mother centrioles (arrow). 3D-structured illumination microscopy images distinguish the mother centriole from the daughter (the daughter grows from the side of the mother) and show that GFP-Root localizes at the entrance to the mother centriole lumen. In spermatids, GFP-Root localizes to the proximal end of the centriole (arrows). γ-Tub and Bld10 mark the centrioles. (C) GFP-Root localizes asymmetrically to NB centrosomes: higher at the mother than the daughter. The mother and daughter centrosomes are distinguished by higher level of the pericentriolar material protein Cnn at the daughter. Phospho-Histone H3 (pH3) marks the mitotic cells. (D) Representative images showing distributions of GFP-Root, Cnn, γ-Tub, Plp, and Bld10 in NB centrosomes. Cnn or γ-Tub that distributes significantly more to daughter centrosomes is used to distinguish the mother and daughter centrosomes. (E) Quantification of asymmetric distribution of proteins between the mother and the daughter centrosomes in NBs. Total signal intensity of the mother plus the daughter centrosome is 100%. The distribution of protein in the daughter or the mother centrosome was calculated as $100\% \times D/(D + M)$ or $100\% \times M/(D + M)$, where D was the signal intensity in the daughter centrosome and M was the intensity in the mother. Numbers of NBs measured are indicated in the bars. Bars: (A–C) 10 µm; (B and C, zoom) 500 nm; (D) 500 nm. See also Fig. S4.

type (Fig. 8, A–C). In mammalian cells, apart from localizing at rootlets in ciliated cells, Root also assembles fibrous linkers between the centriole pairs in premitotic cells, linking the proximal ends of the mother centrioles of each pair (Bahe et al., 2005; Yang et al., 2006). C-Nap1 resides at the proximal end of mother centrioles, and also daughter centrioles, but only when the daughters are separated from their mothers ("disengaged" state, typically in late M and G1 phases; Mayor et al., 2000, 2002). Although high-throughput expression data indicated a high expression of Root mRNAs in testes and a low expression in larval brains (FlyBase; St Pierre et al., 2014), endogenous Root was not detected at centrosomes in testis or larval brains with affinity-purified Root antibody (Fig. S4, A and B). No apparent alternative splice products of Root were reported in testis to account for a lack of detection with our antibody, but it is possible that the antibody does not recognize epitopes because of posttranslational modifications or inaccessibility. However, ectopically expressed GFP-Root localized to the centrioles or centrosomes in these tissues. During spermatogenesis, GFP-Root associated with centrioles, but the localization patterns varied by developmental stages. In polar spermatocytes, GFP-Root localized to fibers that connected the two centriole pairs (Fig. 8 B), similar to Root in mammalian cells. However, in G2 phase mature spermatocytes, where there are two mother-daughter–engaged centriole pairs, GFP-Root localized at the base of the mother but not the daughter centriole, similar to C-Nap1 in mammalian cells. In spermatids, GFP-Root localized to the proximal end of the single centriole (Fig. 8 B). The mutant RFP-RootDEL localized in a similar pattern in testis as GFP-Root (Fig. S4 C). Thus, even though there is no detectable endogenous Root in *Drosophila* testes, ectopically expressed Root exhibits localization patterns that reflect those of mammalian Root and C-Nap1.

During asymmetric division of the neuroblast (NB) in larval brains, the daughter centrosome (with the younger centriole) in interphase retains MT-organizing center activity and is inherited by the self-renewed NB, whereas the mother centrosome in interphase loses its PCM until mitosis and is then segregated into the differentiating ganglion mother cell (GMC; Januschke et al., 2011). Several centrosomal proteins localize asymmetrically to the daughter centrosome (Cnn, γ-Tub, and Centrobin) most prominently at interphase, whereas others distribute equally (e.g., Bld10), or, in the case of Plp, enriches slightly more in the mother (Januschke et al., 2013; Lerit and Rusan, 2013; Fig. 8, D and E). When ectopically expressed in NBs, GFP-Root and mutant RFP-RootDEL localized asymmetrically, with significantly higher accumulation at the mother than the daughter centrosome (Fig. 8, C–E; and Fig. S4 D), making them unique mother centrosome markers in NBs.

Bld10 is required for GFP-Root localization to brain and testis centrosomes/centrioles but is dispensable for Rootlet assembly in ciliated neurons

Studies in mammalian cells showed that Bld10 (CEP135) recruits C-Nap1 to regulate centrosome cohesion during the cell cycle (Kim et al., 2008). In accordance with this, we found that in *bld10* mutant larval brains, ectopic GFP-Root failed to localize to centrosomes in NBs and ganglion mother cells (Fig. 9 A); similarly, GFP-Root localization at centrioles in mature spermatocytes and spermatids was also blocked (Fig. 9 B). However, Bld10 was not required for Root localization to rootlets in ciliated neurons, and *bld10* mutants appeared capable of organizing normal rootlets (Fig. 9 C). Indeed, this is consistent with the observation that, unlike *Root* mutants, *bld10* flies have normal locomotor performance (Fig. 9 D). Conversely, Bld10 localization to basal bodies in olfactory neurons was not affected by *Root*[66] (Fig. S5).

Discussion

Here we show that *Drosophila* Root organizes rootlets at the base of primary cilia in sensory neurons and is essential for sensory neuron functions, including negative geotaxis, taste, touch response, and hearing. A recent study of Root loss of function using RNAi knockdown in *Drosophila* also showed the essential role for Root in sensory perception of Ch neurons (Styczynska-Soczka and Jarman, 2015). We show that Root is not required for normal cilium assembly, and it is likely that the required neuronal function of Root is at the rootlets, as rescue constructs that express tagged versions of Root rescued phenotypes completely or partially, and partial rescue coincided with assembly of smaller rootlets. Root was required for cohesion of the basal body pair in ciliated neurons, and centrioles, but not cilia, were required for rootlet assembly. Furthermore, the conserved Root domain is required for rootlet formation and for Root function, but not for localization to basal bodies. Bld10, a presumptive Root partner (Kim et al., 2008), was not required for Root assembly into rootlets in sensory neurons but was required for ectopic Root localization to the proximal base of the centriole at the threshold of the lumen. In addition, ectopic Root localized asymmetrically in NBs, accumulating much more at the mother centrosome.

Rootlet and ciliary function
How do rootlets affect sensory neuron function? Because rootlets appear to always be associated with cilia, it is likely that rootlets support the structure and/or functions of cilia, enabling their role as sensors of environmental cues. However, *Root* mutant mice, which lack rootlets, develop normally, and during development Root is not essential for normal cilium functions, including environmental perception and cilium beating (Yang et al., 2005); however, the long-term stability of cilia requires Root (Yang et al., 2005). One important consideration for the mouse phenotypes is that the paralog, C-Nap1, may have redundant functions with Root. Indeed, in our study, we found that even very small rootlets, resembling the localization of C-Nap1 at the base of centrioles, could rescue *Root*[66]. How can the rootlet, and especially a short rootlet, support mechanosensation? It has been proposed that a cytoskeletal structure (e.g., possibly the rootlet cytoskeleton) links mechanosensation from extracellular forces via the dendrite to the axon or synapse (Gillespie and Walker, 2001). Because the rootlet does not span across the neuron from the basal body to the axon, perhaps it links to another cytoskeleton like MTs. The conserved Root domain, which we show is essential for Root function but not localization to basal bodies, interacts with several kinesin light chains (Yang and Li, 2005), supporting the idea of a possible linkage between the rootlet and the MT cytoskeleton.

In *C. elegans*, *che-10* (*Root* orthologue) mutants show much more severe defects, with cilium, transition zone, and basal body degeneration during development due to severe defects in intraflagellar transport and preciliary membrane disrup-
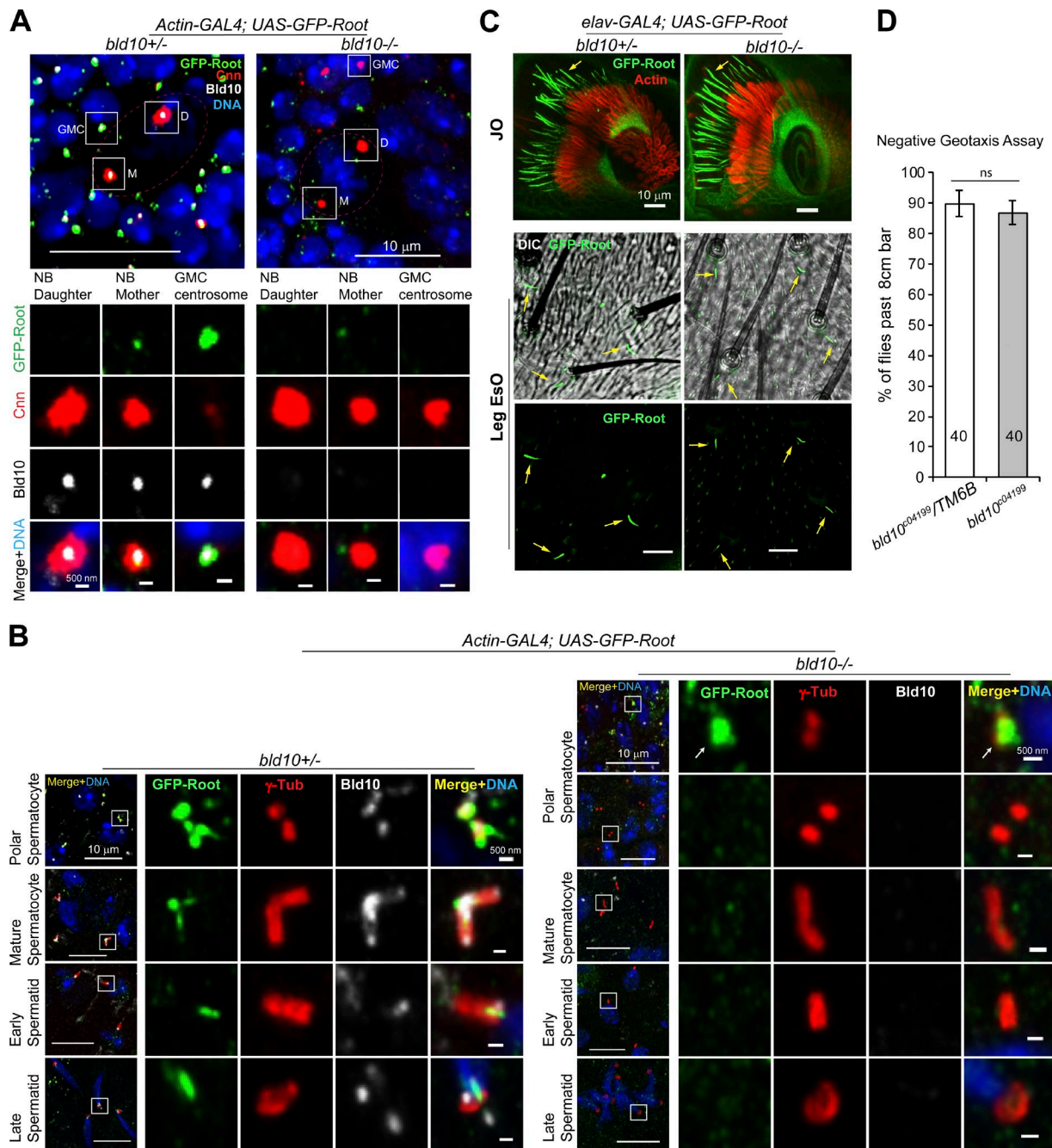
Figure 9. **Bld10 is required for GFP-Root localization to brain and testis centrosomes/centrioles but is dispensable for rootlet assembly in ciliated neurons.** (A) *bld10* null mutant abolishes GFP-Root localization to centrosomes in NBs and ganglion mother cells (GMCs). The mother and the daughter centrosomes in the NB are distinguished by the pericentriolar material protein Cnn, which distributes more in the daughter than the mother. (B) *bld10* mutant abolishes GFP-Root localization to centrioles in mature spermatocytes and spermatids, though some polar spermatocytes still have GFP-Root localizing at the centrioles (arrows). γ-Tub marks the centrioles. (C) In the *bld10* JO or leg EsOs, GFP-Root localization to rootlets appears unaffected, with normal length and morphology (arrows). Actin marks scolopale rods. (D) *bld10* (null) mutant flies show normal climbing activities in the negative geotaxis assay. Numbers of males assayed are indicated inside the bars. ns, P > 0.05. Bars: (A and B) 10 µm; (zoom) 500 nm; (C) 10 µm. See also Fig. S5.

tion that affects delivery of basal body and ciliary components (Mohan et al., 2013). But these defects may not necessarily be attributed to the rootlet structure because unlike in mammalian cells, CHE-10 also localizes within the basal body and the transition zone (a "nonfilament form" of CHE-10) in neurons both with and without rootlets (Mohan et al., 2013). Moreover, in *che-10* mutants, cilium degeneration also occurs in neurons without rootlets. Thus, in *C. elegans*, CHE-10, which is

required for sensory neuron function, may have acquired new functions that have deviated from its function in mammals and *Drosophila* where Root is restricted to the Rootlet and the proximal base of centrioles.

We found that in *Drosophila* the loss of rootlets impairs sensory neuron functions. Interestingly, the size of rootlets appears to affect neuronal function, particularly in ChOs that normally have long rootlets, because we observed that short-

ened rootlets, resulting serendipitously from GFP-Root expression in the *Root[66]* mutant background, only partially restored the JO hearing impairment.

The morphologically normal appearance and stability of cilia in *Root[66]* neurons indicate that rootlets may mediate signal transduction from cilia to the cell body, perhaps as a key structural element of the mechanoreceptor. Shorter rootlets may transduce signal less efficiently than longer ones in the JO, explaining why GFP-Root did not completely rescue the *Root[66]* phenotype. Alternatively, rootlets may be important for ciliary protein trafficking at the base of the cilium and between the dendrite and the cilium. In this scenario, long rootlets may support trafficking along the dendrite more efficiently than short ones. If this is the case, defective trafficking must be limited because loss of intraflagellar transport trafficking would result in failure to maintain the cilium structure and produce a more severe uncoordination phenotype (Han et al., 2003; Sarpal et al., 2003).

Root function in mitotic centrosomes

With ectopic Root expression, we showed that in a *Drosophila* cell line without cilia or rootlets, Root organized rootlet-like structures extending from the centrioles. However, ectopically expressed Root in cells such as NBs, spermatocytes, and spermatids localized to a smaller focus in the centrioles/centrosomes. In Ch neurons, Root assembles into longer rootlets than in Es neurons. It will be interesting to know what determines the forms of Root protein (centrosomal form vs. rootlet form), and in the case of rootlets, what defines their length. How Root is targeted to basal bodies and how the Root domain regulates rootlet assembly remain important questions.

Root, like its mammalian orthologue C-Nap1, specifically associates with mother centrioles upon ectopic expression in testes or NBs. We determined that centriolar localization of Root in NBs and testes requires the proximal centriolar protein Bld10, yet Bld10 is not required for Root localization to rootlets in ciliated neurons. Therefore, different mechanisms may regulate the recruitment of Root to centrioles in proliferating cells versus rootlet assembly at basal bodies in ciliated neurons.

Overall, our study shows that *Drosophila* Root is a key structural component of ciliary rootlets that assembles in a centriole-dependent manner, and ciliary rootlets are necessary for neuronal sensory functions.

Materials and methods

Molecular cloning

Root rescue construct (7,398 bp) is the genomic sequence ranging from the beginning of the first coding exon (exon2) to the end of the last coding exon (exon 10, excluding the stop codon). It was generated by ligating together three sequence fragments (fragments 1–3) cloned from *Root* genomic DNA (BAC clone: RP98-29F6; Fig. 1 A). The fragments were cloned into pGEM-T Easy Vector system (Promega) individually, which were followed by "cut and paste" ligation: Fragment 2 and fragment 3 were first ligated together through a Pac I site, and fragment 1 was then ligated 5′ of fragment 2 through a unique EcoRI site (Fig. 1 A). The entire rescue construct fragment was then cloned into BamHI and NotI sites of the Gateway vector pENTR-2B (Invitrogen).

RootDEL (6169 bp) is the genomic sequence beginning right after the end of Root conserved domain (amino acid 334) to the end of the last coding exon (exon 10, excluding the stop codon). It was cloned similar to *Root*, except that fragment 1 in *RootDEL* starts with DNA

sequence encoding the amino acid 334 of the Root protein. The entire *RootDEL* sequence was then cloned into Sal I and Not I sites of the Gateway vector pENTR-2B.

p*UASp-GFP-Root*, p*UASp-Myc-Root*, and p*UASp-RFP-RootDEL* were created through Gateway cloning into the pPGW-attB, pPMW-attB, and pPRW-attB vectors, respectively. pPGW-attB, pPMW-attB, and pPRW-attB vectors were constructed by cloning a 368-bp fragment containing *attB* sequence from pVALIUM1 (2,567–2,935 bp) into the NsiI restriction site (at 710-bp position in all three vectors) of pPGW, pPMW, and pPRW, respectively. pPGW, pPMW, and pPRW are insect expression Gateway destination vectors under the control of the *UASp* promoter and with EGFP, 6xMyc, and RFP as fusion tags on the N terminus of the target protein, respectively. They are obtained from Terence Murphy's *Drosophila* Gateway Vector Collection at Carnegie Institution of Washington.

Primers used in the study are listed as follows: *attB*: forward, 5′-CCAATGCATGGCTGCATCCAACGCGT-3′, reverse, 5′-CCA ATGCATAATTAGGCCTTCTAGTGG-3′; *Root-Fragment 1*: forward, 5′-GGATCCGATGCAGGCGTATCGCGATAACT-3′, reverse, 5′-ATC ACTGCTCAGATTCTCGAACTACAAG-3′; *Root-Fragment 2*: forward, 5′-GTAATTATTTCTAAAAGCTGTCAGTGGGC-3′, reverse, 5′-GCAGCTCCTGCTTCCGGATGCATTCCTCC-3′; *Root-Fragment 3*: forward, 5′-GGTGCAGATGCGCACCAAGGAGGAGGAG-3′, reverse, 5′-TCGAGTCGACGCGGCCGCGAATCGCGATCATAG TCCCGGCAGC-3′, *RootDEL-Fragment 1*: forward, 5′-AAGTCGAC CCAATGGCTCCAACGCAACGGTCGCC-3′, reverse, 5′-ATC ACTGCTCAGATTCTCGAACTACAAG-3′; and PCR genotyping: forward, 5′-GGCAGTGGAGCTGGAGATCCAACGTATACTG-3′, reverse, 5′-CCACGATCCCGGGTGACGCAGGCCAAGTC-3′.

Fly genetics

p*UASp*-GFP-Root, p*UASp*-Myc-Root, and p*UASp*-RFP-RootDEL transgenic flies were made by GenetiVision Inc. via PhiC31-mediated chromosome integration on the second chromosome, with VK37:(2L)22A3 as the docking site for p*UASp*-GFP-Root, and VK1:(2R)59D3 for p*UASp*-Myc-Root and p*UASp*-RFP-RootDEL.

Root[66] allele was obtained from screening by the *Drosophila* TILLING project at the University of Washington (Henikoff et al., 2004; Cooper et al., 2008). An ~1.5-kb sequence in the root genomic region was screened for DNA sequence changes. Unfortunately, the TILLING service is no longer available for *Drosophila*. *Root[66]* has a nonsense mutation acquired from ethyl methanesulfonate mutagenesis that leads to a protein truncation in the beginning of exon 5 (Fig. 1 A), and the *Root[66]* stock was backcrossed for nine generations against a *w[1118]* background. Stocks bearing *Root[MB08356]* and *Df(3R)Exel6197* were obtained from the Bloomington Drosophila Stock Center (BDSC), and *Root[KK102209]VIE-260B* (RNAi construct) was obtained from the Vienna *Drosophila* Resource Center. Throughout this study, we used *Df(3R)Exel6197* as a deficiency for *Root* and designated it as "*Df*", and *w[1118]* or *Root[66]/TM6B* or *Df/TM6B* as controls.

Fly strains used in the study are listed as follows: *w[1118]* (FBal0018186); *Root[66]* (chr 3; this study; Drosophila TILLING Service); *Df(3R)Exel6197* (chr 3; BDSC 7676; FBst0007676); *Root[MB08365]* (chr 3; BDSC 26368; FBst0026368); *UAS-Root-RNAi* (chr 2; Vienna Drosophila RNAi Center v110171); p*UAS-GFP-Root* (chr 2; this study); p*UAS-Myc-Root* (chr 2; this study); p*UAS-RFP-RootDEL* (chr 2; this study); *tubp-GAL4[LL7]* (chr 3; BDSC 5138; FBst0005138; Lee and Luo, 1999); *Act5C-GAL4[E1]* (chr 2; BDSC 25374; FBst0025374; Sedat, 2008); *elav-GAL4[C155]* (chr X; BDSC 458; FBst0000458; Lin and Goodman, 1994); *JO15-2-GAL4* (chr 2; Eberl Laboratory; Sharma et al., 2002); *tilB-GAL4, nan-GAL4* (chr 2; Eberl Laboratory); *Insc-GAL4* (chr 2; BDSC 8751; FBst0008751); *wor-GAL4* (chr 2; BDSC 56553;

FBst0056553); *nos-GAL4-VP16* (chr 3; BDSC 4937; FBst0004937); *Chibby-Tomato* (chr 3; Enjolras et al., 2012); *GFP-CG11356* (chr X; Enjolras et al., 2012); *Ana 1-GFP* (chr 2; Blachon et al., 2009); *Sas-4^{S2214}* (chr 3; BDSC 12119; FBst0012119; Basto et al., 2006); *UAS-mCD8-GFP^{LL5}* (chr 2; BDSC 5173; FBst0005137); *UAS-mCD8-RFP* (chr 3; BDSC 27399; FBst0027399); *Sas-6^{c02901}* (chr 3; BDSC 11148; FBst0011148); *Plp^{s2172}* (chr 3; BDSC 12089; FBst0012089); *spd-2^{z3-3316}* (chr 3; FBal0240471; Giansanti et al., 2008); *Df(3L)Brd15*, *Df* for *Plp* (chr 3; BDSC 5354; FBst0005354); *Df(3L)st-j7*, *Df* for *spd-2* (chr 3; BDSC 5416; FBst0005416); *asl^2* (chr 3; Varmark et al., 2007); *asl^3* (chr 3; Varmark et al., 2007); *cnn^{hk21}* (chr 2; BDSC 5039; FBst0005039); *cnn^{25cn1}* (chr 2; Zhang and Megraw, 2007); *bld10^{c04199}* (chr 3; FBst1007073; Mottier-Pavie and Megraw, 2009); and *bld10^{f01951}* (chr 3; FBst1017382; Mottier-Pavie and Megraw, 2009).

Production of the Root antibody

DNA sequence encoding amino acids 198–440 of Root were cloned into the pET100/DTOPO vector (Invitrogen) for expression of 6xHis-tagged Root protein fragment in *Escherichia coli* strain BL21(DE3) pLysE. The 6xHis-tagged protein was then purified by Ni^{2+}-immobilized metal affinity chromatography and used to immunize rabbits (Cocalico Biologicals). For affinity-purified antibodies, the rabbit serum was affinity-purified against the antigen bound to a strip of UltraCruz 0.45-µm pore size nitrocellulose membrane (Santa Cruz Biotechnology).

Western blotting

Each lane of a 7.5% SDS-PAGE gel was loaded with lysates from ∼40–50 antenna pairs or three ovary pairs. Antennae were dissected, chopped into small pieces using a razor blade, then grinded and lysed in SDS loading buffer and boiled at 98°C for 10 min. Ovaries were directly lysed in SDS loading buffer and then boiled at 98°C for 10 min. Proteins were separated using an SDS-PAGE mini-gel electrophoresis system (Bio-Rad) and transferred to UltraCruz 0.45-µm pore size nitrocellulose membrane (Santa Cruz Biotechnology) using Trans-Blot SD Semi-Dry Transfer system (Bio-Rad). The membrane was probed with rabbit anti–Root serum (1:5,000) and mouse anti–α-tubulin antibody (DM1A, 1:20,000; Sigma-Aldrich). For secondary antibodies, IRDye800CW Goat anti-mouse antibody and IRDye680LT Goat anti-rabbit antibody (LI-COR Biosciences) were used. The membrane was scanned with an Odyssey Infrared Imaging System (LI-COR Biosciences).

Immunohistochemistry and microscopy

For the staining of brains and testes, larval brains or testes from adult males were dissected in Dulbecco's PBS (DPBS; Invitrogen), then transferred to a 4-µl drop of DPBS on a slide and then covered with a siliconized coverslip containing 1 µl 18.5% formaldehyde (Millipore) in DPBS. After the tissue was allowed to flatten for 20–30 s under the weight of the coverslip, the slide was snap-frozen by plunging into liquid nitrogen. The slide was removed from liquid nitrogen and the coverslip was flipped off using a single-edged razor blade and then immersed immediately into −20°C methanol and incubated for 10 min. The slides were then transferred to PBS. A Super PAP Pen (Immunotech) was used to draw a hydrophobic ring around the tissue. The tissues were stained with antibodies in 50 µl of PBS solution containing 5 mg/ml BSA and 0.1% saponin (Sigma-Aldrich).

For the staining of culture cells, Kc167 cells were prepared according to the method described by Kao and Megraw (2004). Cells were incubated on poly-L-lysine (Sigma-Aldrich)–treated slides for 30 min; the slide was then rinsed briefly in PBS and placed directly into −20°C methanol for 10 min. Cells were washed with PBS a few times and stained with antibodies in PBS + 5 mg/ml BSA + 0.1% saponin.

Embryo staining was adapted as previously described (Megraw et al., 1999; Kao and Megraw, 2009). Basically, overnight embryos were dechlorinated in 50% bleach and then fixed in a mixture of methanol and heptane (1:1) for 5–7 min with gentle agitation at room temperature. For phalloidin staining, embryos were fixed with a mixture of heptane and formaldehyde (1:1) and the vitelline membranes were removed manually by rolling the embryos between a frosted slide and coverglass. The fixed embryos were first blocked with PBS + 0.1% Triton X-100 + 5 mg/ml BSA + 0.1% saponin for 1 h and then incubated with antibodies in PBS + 0.1% Triton X-100 + 5 mg/ml BSA + 0.1% saponin for 2 h. After each antibody incubation, embryos were washed three times, 15 min each, with PBS + 0.1% Triton X-100. Embryos were mounted in 80% glycerol on slides.

For the whole-mount staining of antennae and legs, antennae and legs from pharate adults were dissected in DPBS, cut apart (to promote the penetration of solution into the interior tissues surrounded by cuticles) into smaller pieces, and then fixed in in PBS + 3% Triton X-100 + 9% formaldehyde with agitation for 30 min. After a few rinses, the samples were incubated with the primary antibodies and then secondary antibodies in PBS + 3% Triton X-100 + 5 mg/ml BSA + 0.1% saponin at room temperature for 3 h and then at 4°C overnight. After each antibody incubation, the samples were washed for 15 min five times. All washes were in PBS + 0.1% Triton X-100.

For the staining of cryosectioned antennae, antennae were dissected in PBS, fixed in 4% (vol/vol) paraformaldehyde in PBS for 20 min, embedded in OCT (Ted Pella), and then cut into 25-µm sections in a cryostat. The antennal cryosections were then stained with primary and secondary antibodies.

For staining of squashed antennae, antennae were dissected and squashed on Superfrost Plus microscope slides (Thermo Fisher Scientific) and fixed with −20°C methanol for 10 min as described for the staining of testes or larval brains.

For observing native signals from fluorescent proteins and/or the signal from fluorescent-tagged phalloidin staining in whole-mount antennae and legs, antennae or legs were dissected and then fixed in PBS + 0.3% Triton X-100 + 4% formaldehyde for 15 min. After a few quick washes, samples were directly mounted in 80% glycerol on slides. For actin staining of scolopidia, after the fix, samples were incubated with fluorescent-tagged phalloidin in PBS + 0.3% Triton X-100 + 5 mg/ml BSA + 0.1% saponin for 2 h at room temperature, washed, and mounted.

Secondary goat antibodies conjugated to Alexa 488, 568, and 647 (1:200 for cryosections and 1:1,000 for the others; Life Technologies) were used. DNA was stained with DAPI (1 µg/ml; Invitrogen). For confocal imaging, samples were imaged at room temperature using a Nikon A1 confocal microscope equipped with a 60×/NA 1.49 oil immersion objective and NIS-Elements software. For superresolution imaging using 3D-structured illumination microscopy, DeltaVision OMX Blaze (GE Healthcare) was used with an Olympus 60×/NA1.42 oil immersion objective and images were processed with SoftWorx software (GE Healthcare).

After image acquisition, image brightness and contrast as well as color channel separation were processed using Photoshop CS4 (Adobe Systems), following *The Journal of Cell Biology* guidelines, with no changes to gamma settings.

Primary antibodies/dyes used in the study are listed as follows: rabbit anti–Root (serum, 1:1,000; this study), rabbit anti–Root (affinity purified, 1:100; this study), mouse anti–γ-tubulin (GTU88, 1:1,000; Sigma-Aldrich), mouse anti–Myc (9B11, 1:2,000; Cell Signaling Technology), guinea pig anti–Cnn (1:2,000; Megraw Laboratory), rabbit anti–Cnn (1:1,000; Megraw Laboratory), rabbit anti–Plp (1:1,000; gift from N. Rusan, National Heart, Lung, and Blood Institute, National Institutes of Health, Bethesda, MD), mouse anti–GFP (1:1,000; Uni-

versity of California, Davis/National Institutes of Health NeuroMab Facility), chicken anti–GFP (1:1,000; Aves Labs), mouse 22C10 (1:30; Developmental Studies Hybridoma Bank), mouse 21A6 (1:30; Developmental Studies Hybridoma Bank), mouse anti–α-tubulin (DM1A, 1:500; Sigma-Aldrich), Alexa Fluor 546 Phalloidin (1:400; Molecular Probes), Texas red-X phalloidin (1:200; Molecular Probes), phalloidin CruzFluor 405 conjugate (1:1,000; Santa Cruz Biotechnology), mouse anti–phospho-histone H3 (1:1,000, Millipore), rabbit anti–phospho-histone H3 (1:1,000; Millipore), and rabbit anti–RFP (1:1,000; Millipore).

Transmission electron microscopy of adult chordotonal neurons

Dissected fly heads carrying intact antennae were fixed by immersion overnight at 4°C in a fixative containing 2.5% glutaraldehyde and 2% paraformaldehyde in biphosphate buffer at pH 7.2. Heads were post-fixed in osmium tetroxide, treated with uranyl acetate, dehydrated in a graded series of alcohol, and subsequently embedded in epoxy resin. Serial thin sections (60–80 nm) of antennae were cut in a Leica Reichert Ultracut S ultramicrotome, collected on Formvar-coated copper slot grids, and stained with uranyl acetate and lead citrate. Samples were examined and imaged at 80 kV using a Hitachi 7650 electron microscope with AMT 2kX2k digital camera.

Negative geotaxis assay

The assay was modified from Ali et al. (2011). The day before the experiment, ~10 males, aged 3–5 d, were transferred as a group to a fresh vial with food. Right before the assay, flies were transferred without anesthesia into a 20 cm–long clear testing vial. In the assay, flies were gently tapped down to the bottom of the vial and were then given 10 s to climb up the vial. The number of flies that climbed above the 8-cm mark was recorded. After each test, flies were given 1 min to recover. Each group of flies was tested 10 times, and at least three groups of flies were assayed for each genotype.

Larval touch sensitivity assay

The assay was modified from Kernan et al. (1994) and Caldwell et al. (2003). A group of 10 larvae were, one by one, gently touched on their head segments with a human hair during bouts of linear locomotion. A score was assigned to the larva according to its response to the touch: 0, the larva showed no response; 1, the larva showed hesitation with ceased movement; 2, the larva showed anterior contractions with or without turns; 3, the larva showed one full wave of body contractions; 4, the larva showed two or more full waves of body contractions. Each of the 10 larvae was tested with four touches and the four scores were added up to a total score; at least three groups of larvae were assayed for each genotype.

Proboscis extension reflex assay

The method was modified according to the method of Shiraiwa and Carlson (2007). Flies that were 2–3 d old were starved for 16–20 h in vials with cotton soaked in water. Right before the assay, flies were anesthetized on ice and each fly was quickly glued down on its back to a 22 × 22–mm coverslip with melted myristic acid (TCI America). Flies were first sated with water, then touched on their front legs with a drop of sucrose solution, and the proboscis extension reflex responses (yes or no) were recorded. About 15–20 flies in each group were tested with a series of sucrose solutions ranging in concentrations from 1 μM to 1 M; at least three groups of flies were assayed for each genotype. Flies that escaped were omitted from the experiment.

Electrophysiological recording of SEPs

Auditory recordings were conducted as described in detail elsewhere (Eberl et al., 2000; Eberl and Kernan, 2011). Each fly was mounted in a

200-μl pipette tip trimmed such that only the head protruded. The neck was immobilized with plasticine. The computer-generated pulse component of the *Drosophila* courtship song was played through a speaker and the sound was transported through a Tygon tube (Fisher Scientific) placed at a distance of 1 mm from the fly's head. The sound stimulus intensity was measured at 5.3 mm/s at the position of the antennae, using a calibrated Emkay NR3158 particle velocity microphone (Knowles). Two tungsten electrodes were used: The recording electrode was inserted at the joint between the first and second antennal segment from a dorsofrontal direction, and the reference electrode was inserted in the head cuticle. The signals were amplified by a DAM50 differential amplifier (WPI) and digitized and normalized using Superscope II software (GW Instruments).

Male fertility test

Virgin w^{1118} females and newly eclosed males were collected and held apart for 3–5 d before mating. In each test, a single male was mated with a single w^{1118} virgin female for 4 d. The crosses were then examined a few days later to see whether they produced any progenies (larvae). The whole test was conducted at 25°C.

Tail length measurements of mature sperm

The mature sperm were prepared and measured as previously described (Chen and Megraw, 2014). Seminal vesicles from males older than 10 d were dissected in media with 1 μg/ml Hoechst 33342 dye (Sigma-Aldrich) and were poked to release mature sperm. Individual sperm were imaged at room temperature with an Eclipse TE2000-U inverted microscope equipped with a Plan Fluor 10× NA 0.30 phase contrast objective (Nikon), the NIS-Elements software (Nikon), and a ORCA-AG digital camera (Hamamatsu Photonics). The length of the tail was measured using the NIS-Elements software. Approximately 10 sperm were measured from each pair of testes, and at least three pairs of testes were assessed for each genotype.

Cell culture

Drosophila Kc167 cells (Cherbas et al., 1988) were maintained in Hyclone CCM3 medium (Thermo Fisher Scientific) supplemented with 5% fetal bovine serum (Omega Scientific) and penicillin-streptomycin (100 IU/ml penicillin and 100 μg/ml streptomycin; Corning). Cells were cotransfected with p*UAS-GFP-Root* and pMT-GAL4 (Drosophila Genomics Resource Center) using lipofectamine 2000 (Invitrogen) and the protein expression was induced with 1 mM Cu_2SO_4 20–24 h later. Cells were prepared for immunostaining 20–24 h after induction.

Analysis of the asymmetric distribution of centrosomal proteins

Larval brains were stained as described in the online supplemental material. Phospho-Histone H3 staining signals were used to determine the stage of mitosis, and the intensities of protein signals from the mother and the daughter centrosomes within the same cell were measured with subtraction of the cytoplasmic background, using the software ImageJ (IJ 1.46r). The distribution of protein in the daughter or the mother centrosome was calculated as $100\% \times D/(D + M)$ or $100\% \times M/(D + M)$, where D was the signal intensity in the daughter centrosome, and M was the intensity in the mother.

Statistics

For all graphs in this article, error bars represent standard error of the mean. Unless otherwise stated, a two-tailed unpaired Student's t test was used to determine the statistical significance: ns, $P > 0.05$; *, $P \leq 0.05$; **, $P \leq 0.01$; ***, $P \leq 0.001$; ****, $P \leq 0.0001$.

Online supplemental material

Video 1 shows that *Root[66]* mutant flies have severe defects in startle response. Fig. S1 shows homology of the Root conserved domain in Root and C-Nap1 across species. Fig. S2 shows that in *Root[66]* mutant neurons, GFP-Root expression forms rootlets with normal length in Es organs but organizes shorter ones in ChOs. Fig. S3 shows the rootlet assembly in different centriolar/centrosomal mutants. Fig. S4 shows endogenous Root is undetectable in testes or larval brains, and ectopic RFP-RootDEL localizes to centrioles or centrosomes in testes and larval brains. Fig. S5 shows Bld10 localization to centrioles is unaffected in *Root[66]* mutant olfactory neurons. Online supplemental material is available at http://www.jcb.org/cgi/content/full/jcb.201502032/DC1. Additional data are available in the JCB DataViewer at http://dx.doi.org/10.1083/jcb.201502032.dv.

References

Ali, Y.O., W.Escala, K.Ruan, and R.G.Zhai. 2011. Assaying locomotor, learning, and memory deficits in *Drosophila* models of neurodegeneration. *J. Vis. Exp.*49:2504.

Bahe, S., Y.D.Stierhof, C.J.Wilkinson, F.Leiss, and E.A.Nigg. 2005. Rootletin forms centriole-associated filaments and functions in centrosome cohesion. *J. Cell Biol.*171:27–33. http://dx.doi.org/10.1083/jcb.200504107

Basto, R., J.Lau, T.Vinogradova, A.Gardiol, C.G.Woods, A.Khodjakov, and J.W.Raff. 2006. Flies without centrioles. *Cell.*125:1375–1386. http://dx.doi.org/10.1016/j.cell.2006.05.025

Blachon, S., X.Cai, K.A.Roberts, K.Yang, A.Polyanovsky, A.Church, and T.Avidor-Reiss. 2009. A proximal centriole-like structure is present in *Drosophila* spermatids and can serve as a model to study centriole duplication. *Genetics.*182:133–144. http://dx.doi.org/10.1534/genetics.109.101709

Caldwell, J.C., M.M.Miller, S.Wing, D.R.Soll, and D.F.Eberl. 2003. Dynamic analysis of larval locomotion in *Drosophila* chordotonal organ mutants. *Proc. Natl. Acad. Sci. USA.*100:16053–16058. http://dx.doi.org/10.1073/pnas.2535546100

Carvalho-Santos, Z., P.Machado, I.Alvarez-Martins, S.M.Gouveia, S.C.Jana, P.Duarte, T.Amado, P.Branco, M.C.Freitas, S.T.Silva, et al.2012. BLD10/CEP135 is a microtubule-associated protein that controls the formation of the flagellum central microtubule pair. *Dev. Cell.*23:412–424. http://dx.doi.org/10.1016/j.devcel.2012.06.001

Chen, J.V., and T.L.Megraw. 2014. Spermitin: a novel mitochondrial protein in *Drosophila* spermatids. *PLoS ONE.*9:e108802. http://dx.doi.org/10.1371/journal.pone.0108802

Cherbas, P., L.Cherbas, S.S.Lee, and K.Nakanishi. 1988. 26-[125I]iodoponasterone A is a potent ecdysone and a sensitive radioligand for ecdys-

one receptors. *Proc. Natl. Acad. Sci. USA.*85:2096–2100. http://dx.doi.org/10.1073/pnas.85.7.2096

Cooper, J.L., B.J.Till, and S.Henikoff. 2008. Fly-TILL: reverse genetics using a living point mutation resource. *Fly (Austin).*2:300–302. http://dx.doi.org/10.4161/fly.7366

Dix, C.I., and J.W.Raff. 2007. *Drosophila* Spd-2 recruits PCM to the sperm centriole, but is dispensable for centriole duplication. *Curr. Biol.*17:1759–1764. http://dx.doi.org/10.1016/j.cub.2007.08.065

Eberl, D.F., and G.Boekhoff-Falk. 2007. Development of Johnston's organ in *Drosophila*. *Int. J. Dev. Biol.*51:679–687. http://dx.doi.org/10.1387/ijdb.072364de

Eberl, D.F., and M.J.Kernan. 2011. Recording sound-evoked potentials from the *Drosophila* antennal nerve. *Cold Spring Harb Protoc.*2011:t5576. http://dx.doi.org/10.1101/pdb.prot5576

Eberl, D.F., R.W.Hardy, and M.J.Kernan. 2000. Genetically similar transduction mechanisms for touch and hearing in *Drosophila*. *J. Neurosci.*20:5981–5988.

Enjolras, C., J.Thomas, B.Chhin, E.Cortier, J.L.Duteyrat, F.Soulavie, M.J.Kernan, A.Laurençon, and B.Durand. 2012. *Drosophila* chibby is required for basal body formation and ciliogenesis but not for Wg signaling. *J. Cell Biol.*197:313–325. http://dx.doi.org/10.1083/jcb.201109148

Fawcett, D.W., and K.R.Porter. 1954. A study of the fine structure of ciliated epithelia. *J. Morphol.*94:221–281. http://dx.doi.org/10.1002/jmor.1050940202

Foelix, R.F., R.F.Stocker, and R.A.Steinbrecht. 1989. Fine structure of a sensory organ in the arista of *Drosophila melanogaster* and some other dipterans. *Cell Tissue Res.*258:277–287. http://dx.doi.org/10.1007/BF00239448

Galletta, B.J., R.X.Guillen, C.J.Fagerstrom, C.W.Brownlee, D.A.Lerit, T.L.Megraw, G.C.Rogers, and N.M.Rusan. 2014. *Drosophila* pericentrin requires interaction with calmodulin for its function at centrosomes and neuronal basal bodies but not at sperm basal bodies. *Mol. Biol. Cell.*25:2682–2694. http://dx.doi.org/10.1091/mbc.E13-10-0617

Gallio, M., T.A.Ofstad, L.J.Macpherson, J.W.Wang, and C.S.Zuker. 2011. The coding of temperature in the *Drosophila* brain. *Cell.*144:614–624. http://dx.doi.org/10.1016/j.cell.2011.01.028

Gargano, J.W., I.Martin, P.Bhandari, and M.S.Grotewiel. 2005. Rapid iterative negative geotaxis (RING): a new method for assessing age-related locomotor decline in *Drosophila*. *Exp. Gerontol.*40:386–395. http://dx.doi.org/10.1016/j.exger.2005.02.005

Giansanti, M.G., E.Bucciarelli, S.Bonaccorsi, and M.Gatti. 2008. *Drosophila* SPD-2 is an essential centriole component required for PCM recruitment and astral-microtubule nucleation. *Curr. Biol.*18:303–309. http://dx.doi.org/10.1016/j.cub.2008.01.058

Gillespie, P.G., and R.G.Walker. 2001. Molecular basis of mechanosensory transduction. *Nature.*413:194–202. http://dx.doi.org/10.1038/35093011

Goetz, S.C., and K.V.Anderson. 2010. The primary cilium: a signalling centre during vertebrate development. *Nat. Rev. Genet.*11:331–344. http://dx.doi.org/10.1038/nrg2774

Han, Y.G., B.H.Kwok, and M.J.Kernan. 2003. Intraflagellar transport is required in *Drosophila* to differentiate sensory cilia but not sperm. *Curr. Biol.*13:1679–1686. http://dx.doi.org/10.1016/j.cub.2003.08.034

Henikoff, S., B.J.Till, and L.Comai. 2004. TILLING. Traditional mutagenesis meets functional genomics. *Plant Physiol.*135:630–636. http://dx.doi.org/10.1104/pp.104.041061

Hildebrandt, F., T.Benzing, and N.Katsanis. 2011. Ciliopathies. *N. Engl. J. Med.*364:1533–1543. http://dx.doi.org/10.1056/NEJMra1010172

Hyams, J.S., and G.G.Borisy. 1975. Flagellar coordination in *Chlamydomonas reinhardtii*: isolation and reactivation of the flagellar apparatus. *Science.*189:891–893. http://dx.doi.org/10.1126/science.1098148

Januschke, J., S.Llamazares, J.Reina, and C.Gonzalez. 2011. *Drosophila* neuroblasts retain the daughter centrosome. *Nat. Commun.*2:243. http://dx.doi.org/10.1038/ncomms1245

Januschke, J., J.Reina, S.Llamazares, T.Bertran, F.Rossi, J.Roig, and C.Gonzalez. 2013. Centrobin controls mother-daughter centriole asymmetry in *Drosophila* neuroblasts. *Nat. Cell Biol.*15:241–248. http://dx.doi.org/10.1038/ncb2671

Jarman, A.P.2002. Studies of mechanosensation using the fly. *Hum. Mol. Genet.*11:1215–1218. http://dx.doi.org/10.1093/hmg/11.10.1215

Kamikouchi, A., H.K.Inagaki, T.Effertz, O.Hendrich, A.Fiala, M.C.Göpfert, and K.Ito. 2009. The neural basis of *Drosophila* gravity-sensing and hearing. *Nature.*458:165–171. http://dx.doi.org/10.1038/nature07810

Kao, L.R., and T.L.Megraw. 2004. RNAi in cultured *Drosophila* cells. *Methods Mol. Biol.*247:443–457.

Kao, L.R., and T.L.Megraw. 2009. Centrocortin cooperates with centrosomin to organize *Drosophila* embryonic cleavage furrows. *Curr. Biol.*19:937–942. http://dx.doi.org/10.1016/j.cub.2009.04.037

Kernan, M., D.Cowan, and C.Zuker. 1994. Genetic dissection of mechanosensory transduction: mechanoreception-defective mutations of *Drosophila*. *Neuron.*12:1195–1206. http://dx.doi.org/10.1016/0896-6273(94)90437-5

Kim, K., S.Lee, J.Chang, and K.Rhee. 2008. A novel function of CEP135 as a platform protein of C-NAP1 for its centriolar localization. *Exp. Cell Res.*314:3692–3700. http://dx.doi.org/10.1016/j.yexcr.2008.09.016

Lechtreck, K.F., and M.Melkonian. 1991. Striated microtubule-associated fibers: identification of assemblin, a novel 34-kD protein that forms paracrystals of 2-nm filaments in vitro. *J. Cell Biol.*115:705–716. http://dx.doi.org/10.1083/jcb.115.3.705

Lee, T., and L.Luo. 1999. Mosaic analysis with a repressible cell marker for studies of gene function in neuronal morphogenesis.*Neuron.*22:451–461. http://dx.doi.org/10.1016/S0896-6273(00)80701-1

Lee, E., E.Sivan-Loukianova, D.F.Eberl, and M.J.Kernan. 2008. An IFT-A protein is required to delimit functionally distinct zones in mechanosensory cilia. *Curr. Biol.*18:1899–1906. http://dx.doi.org/10.1016/j.cub.2008.11.020

Lerit, D.A., and N.M.Rusan. 2013. PLP inhibits the activity of interphase centrosomes to ensure their proper segregation in stem cells. *J. Cell Biol.*202:1013–1022.

Lin, D.M., and C.S.Goodman. 1994. Ectopic and increased expression of Fasciclin II alters motoneuron growth cone guidance. *Neuron.*13:507–523. http://dx.doi.org/10.1016/0896-6273(94)90022-1

Martinez-Campos, M., R.Basto, J.Baker, M.Kernan, and J.W.Raff. 2004. The *Drosophila* pericentrin-like protein is essential for cilia/flagella function, but appears to be dispensable for mitosis. *J. Cell Biol.*165:673–683. http://dx.doi.org/10.1083/jcb.200402130

Mayor, T., Y.D.Stierhof, K.Tanaka, A.M.Fry, and E.A.Nigg. 2000. The centrosomal protein C-Nap1 is required for cell cycle-regulated centrosome cohesion. *J. Cell Biol.*151:837–846. http://dx.doi.org/10.1083/jcb.151.4.837

Mayor, T., U.Hacker, Y.D.Stierhof, and E.A.Nigg. 2002. The mechanism regulating the dissociation of the centrosomal protein C-Nap1 from mitotic spindle poles. *J. Cell Sci.*115:3275–3284.

Megraw, T.L., K.Li, L.R.Kao, and T.C.Kaufman. 1999. The centrosomin protein is required for centrosome assembly and function during cleavage in *Drosophila*. *Development.*126:2829–2839.

Mohan, S., T.A.Timbers, J.Kennedy, O.E.Blacque, and M.R.Leroux. 2013. Striated rootlet and nonfilamentous forms of rootletin maintain ciliary function. *Curr. Biol.*23:2016–2022. http://dx.doi.org/10.1016/j.cub.2013.08.033

Mottier-Pavie, V., and T.L.Megraw. 2009. *Drosophila* bld10 is a centriolar protein that regulates centriole, basal body, and motile cilium assembly. *Mol. Biol. Cell.*20:2605–2614. http://dx.doi.org/10.1091/mbc.E08-11-1115

Ni, L., P.Bronk, E.C.Chang, A.M.Lowell, J.O.Flam, V.C.Panzano, D.L.Theobald, L.C.Griffith, and P.A.Garrity. 2013. A gustatory receptor paralogue controls rapid warmth avoidance in *Drosophila*. *Nature.*500:580–584. http://dx.doi.org/10.1038/nature12390

Orgogozo, V., and W.B.Grueber. 2005. FlyPNS, a database of the *Drosophila* embryonic and larval peripheral nervous system. *BMC Dev. Biol.*5:4. http://dx.doi.org/10.1186/1471-213X-5-4

Park, J., J.Lee, J.Shim, W.Han, J.Lee, Y.C.Bae, Y.D.Chung, C.H.Kim, and S.J.Moon. 2013. dTULP, the *Drosophila melanogaster* homolog of tubby, regulates transient receptor potential channel localization in cilia. *PLoS Genet.*9:e1003814. http://dx.doi.org/10.1371/journal.pgen.1003814

Phelps, C.B., and A.H.Brand. 1998. Ectopic gene expression in *Drosophila* using GAL4 system. *Methods.*14:367–379. http://dx.doi.org/10.1006/meth.1998.0592

Rhodenizer, D., I.Martin, P.Bhandari, S.D.Pletcher, and M.Grotewiel. 2008. Genetic and environmental factors impact age-related impairment of negative geotaxis in *Drosophila* by altering age-dependent climbing speed. *Exp. Gerontol.*43:739–748. http://dx.doi.org/10.1016/j.exger.2008.04.011

Rodrigues-Martins, A., M.Bettencourt-Dias, M.Riparbelli, C.Ferreira, I.Ferreira, G.Callaini, and D.M.Glover. 2007. DSAS-6 organizes a tube-like centriole precursor, and its absence suggests modularity in centriole assembly. *Curr. Biol.*17:1465–1472. http://dx.doi.org/10.1016/j.cub.2007.07.034

Sarpal, R., S.V.Todi, E.Sivan-Loukianova, S.Shirolikar, N.Subramanian, E.C.Raff, J.W.Erickson, K.Ray, and D.F.Eberl. 2003. *Drosophila* KAP interacts with the kinesin II motor subunit KLP64D to assemble chordotonal sensory cilia, but not sperm tails. *Curr. Biol.*13:1687–1696. http://dx.doi.org/10.1016/j.cub.2003.09.025

Sedat, J. 2008. Sedat insertions. http://flybase.org/reports/FBrf0205896.html (accessed January 10, 2015).

Sharma, Y., U.Cheung, E.W.Larsen, and D.F.Eberl. 2002. PPTGAL, a convenient Gal4 P-element vector for testing expression of enhancer fragments in drosophila. *Genesis.*34:115–118. http://dx.doi.org/10.1002/gene.10127

Shiraiwa, T., and J.R.Carlson. 2007. Proboscis extension response (PER) assay in *Drosophila*. *J. Vis. Exp.*3:193.

St Pierre, S.E., L.Ponting, R.Stefancsik, and P.McQuilton;FlyBase Consortium. 2014. FlyBase 102--advanced approaches to interrogating FlyBase. *Nucleic Acids Res.*42:D780–D788. http://dx.doi.org/10.1093/nar/gkt1092

Styczynska-Soczka, K., and A.P.Jarman. 2015. The *Drosophila* homologue of Rootletin is required for mechanosensory function and ciliary rootlet formation in chordotonal sensory neurons. *Cilia.*4:9. http://dx.doi.org/10.1186/s13630-015-0018-9

Sun, Y., L.Liu, Y.Ben-Shahar, J.S.Jacobs, D.F.Eberl, and M.J.Welsh. 2009. TRPA channels distinguish gravity sensing from hearing in Johnston's organ. *Proc. Natl. Acad. Sci. U. S. A.*106:13606–13611. http://dx.doi.org/10.1073/pnas.0906377106

Varmark, H., S.Llamazares, E.Rebollo, B.Lange, J.Reina, H.Schwarz, and C.Gonzalez. 2007. Asterless is a centriolar protein required for centrosome function and embryo development in *Drosophila*. *Curr. Biol.*17:1735–1745. http://dx.doi.org/10.1016/j.cub.2007.09.031

Yang, J., and T.Li. 2005. The ciliary rootlet interacts with kinesin light chains and may provide a scaffold for kinesin-1 vesicular cargos. *Exp. Cell Res.*309:379–389. http://dx.doi.org/10.1016/j.yexcr.2005.05.026

Yang, J., X.Liu, G.Yue, M.Adamian, O.Bulgakov, and T.Li. 2002. Rootletin, a novel coiled-coil protein, is a structural component of the ciliary rootlet. *J. Cell Biol.*159:431–440. http://dx.doi.org/10.1083/jcb.200207153

Yang, J., J.Gao, M.Adamian, X.H.Wen, B.Pawlyk, L.Zhang, M.J.Sanderson, J.Zuo, C.L.Makino, and T.Li. 2005. The ciliary rootlet maintains long-term stability of sensory cilia. *Mol. Cell. Biol.*25:4129–4137. http://dx.doi.org/10.1128/MCB.25.10.4129-4137.2005

Yang, J., M.Adamian, and T.Li. 2006. Rootletin interacts with C-Nap1 and may function as a physical linker between the pair of centrioles/basal bodies in cells. *Mol. Biol. Cell.*17:1033–1040. http://dx.doi.org/10.1091/mbc.E05-10-0943

Zhang, J., and T.L.Megraw. 2007. Proper recruitment of gamma-tubulin and D-TACC/Msps to embryonic *Drosophila* centrosomes requires Centrosomin Motif 1. *Mol. Biol. Cell.*18:4037–4049. http://dx.doi.org/10.1091/mbc.E07-05-0474